Remarks/Arguments

Reconsideration of the above-identified application in view of the present amendment is respectfully requested.

By the present amendment, claims 1-3, 12-13, 17-18, 23-24, 26-31, 34, and 36 have been amended, claims 5-6, 8-9, 19-20, and 32-33 have been cancelled, and new claim 55 has been added. Support for new claim 55 can be found at page 85 as well as page 97 of the present application.

Below is a discussion of the 35 U.S.C. §112, second paragraph, rejection of claims 1-3, 5-6, 8-9, 12-13, 17-20, 23-34 and 36, the 35 U.S.C. §112, first paragraph, rejection of claims 1-3, 5-6, 8-9, 12-13, 17-20, 23-34 and 36, and the objection to claim 1.

1. 35 U.S.C. §112, second paragraph, rejection of claims 1-3, 5-6, 8-9, 12-13, 17-20, 23-34 and 36.

Claims 1-3, 5-6, 8-9, 12-13, 17-20, 23-34, and 36 were rejected under 35 U.S.C. §112, second paragraph, as failing to particularly point out and distinctly claim the subject matter which Applicants regard as their invention. The Office Action argues that claims 1-3, 17-18, 29-34, and 36 do not recite specific, active steps.

By the present amendment, claims 1, 17, 29, and 31 have been amended to recite specific, active steps. The Office Action states that the step of "administering an agent" would be an active step. Amended claims 1 and 17 both recite the active step of "administering an agent". Additionally, amended claims 29 and 31 both recite the active step of "screening a library".

Accordingly, Applicants respectively submit that claims 1, 17, 29, and 31 recite specific, active steps and request that the 35 U.S.C. §112, second paragraph, rejection of these claims be withdrawn. Because claims 2-3, 18, 30, 34, and 36 depend either directly or indirectly from claims 1, 17, 29, and 31, Applicants respectively request that the 35 U.S.C. §112, second paragraph, rejection of these claims also be withdrawn. Applicants also respectively submit that the cancellation of claims 32 and 33 by the present amendment renders the 35 U.S.C. §112, second paragraph, rejection of claims 32 and 33 moot.

2. 35 U.S.C. §112, first paragraph, rejection of claims 1-3, 5-6, 8-9, 12-13, 17-20, 23-34 and 36.

Claims 1-3, 5-6, 8-9, 12-13, 17-20, 23-34, and 36 were rejected under 35 U.S.C. §112, first paragraph, as being non-enabling for a method of reducing GAG content in a glial scar and promoting neuronal regeneration. The Office Action argues that the present application, while being enabling for *in vitro* methods of reducing GAG content in a glial scar and promoting neuronal regeneration, does not reasonably provide enablement for corresponding *in vivo* methods because the mouse experiments were terminated before any clinical benefit was shown and the standard for enablement requires support for recovery of function. Additionally, the Office Action argues that the present application, while being enabling for intrathecal and topical administration, does not reasonably provide enablement for other methods of administration (*i.e.*, such as intravenous and intramuscular) because there is uncertainty as to the success of intramuscular or intravenous administration of neuroregenerative agents.

Claim 1 is enabled for in vivo applications because one reasonably skilled in the art could make or use the invention from disclosures in the inventions coupled with information known in the art without undue experimentation. Claim 1, as noted above, has been amended to recite a method of reducing glycosaminoglycan (GAG) content in a glial scar of a mammal. The method includes administering to the glial scar of the mammal an agent that inhibits one or more of the following: the expression of primary proteoglycans; the expression and/or activity of a chain initiation enzyme; and the expression and/or activity of a chain elongation enzyme. The agent is selected from the group consisting of antisense oligonucleotides that bind a nucleic acid sequence encoding proteoglycans, ribozymes, DNA enzymes, RNAi constructs, and small molecules.

The present application provides sufficient information for one reasonably skilled in the art to administer an agent, which inhibits the expression of primary proteoglycans, the expression and/or activity of a chain initiation enzyme, or the expression and/or activity of a chain elongation enzyme, to a glial scar of the mammal to reduce GAG content.

Paragraphs 122+ of the presentation application dislcose various agents as well as method of making such agents that can be used to inhibits the expression of primary proteoglycans, the expression and/or activity of a chain initiation enzyme, or the expression and/or activity of a chain elongation enzyme, to a glial scar of the mammal to reduce GAG content. These agents include antisense oligonucleotides that bind a nucleic acid sequence encoding proteoglycans, ribozymes, DNA enzymes, RNAi constructs, and small molecules. Paragraphs 297+ of the

application teaches that the agents can be administered by various routes including direct injection to the injury site, topical administration, and parenteral. The present application also recognizes that for injuries to the spine or brain, the agent may be administered intrathecally or across the blood brain barrier. Example 8 provides a working example of the administration of an agent intrathecally (i.e., within the spinal canal) using an intrathecally placed tubing. Example 8 also notes that GFP staining of the spinal cord injury site following intrathecal administration of the agent demonstratrated GAG content is decreased. These results are further described in more detail in Grimpe et al. Journal of Neuroscience, Feb. 11, 2004, 24(6); 1393-1397 (a copy of which is attached) Thus, the present application provides a working example of an in vivo decrease in GAG as a result of administering a DNA enzyme.

At the time of the invention, the level of skill in the art was such that in vivo administration of DNA enzymes or interfering RNA to treat nerve tissue was known. The applicant notes J. Lai, M.S. Gold, C.S. Kim, D. Bian, M.H. Ossipov, J.C. Hunter and F. Porreca, Inhibition of neuropathic pain by decreased expression of the tetrodotoxin-resistant sodium channel, NaV1.8, *Pain* **95** (2002), 143–152. (a copy of which is attached). This publication shows that intrathecal administration of antisense oligonucleotides could be effectively administered to a mammal can be used in a therapeutic method to knock down the expression of a gene in nerve cells. Accordingly, the level of skill in the art was sufficiently high such that it would have not required undue experimentation to intrathecally administer DNA enzymes and/or interfering oligonucleotide in vivo to treat a neuronal-tissue. Moreover, the attached memorandum from the applicant also shows that DNA enzymes administered

systemically, in accordance with the present application, by intravenous injection can reduce GAG content at the site of nerve injury. Systemic administration of the agent by intravenous administration is described in application as another possible means of delivering the agent.

In summary, claim 1 is directed to the reduction of GAG content in glial scar of mammals by administering an agent to the glial scars. The present application describes generally various agents and various methods for delivering agent to reduce GAG content in glial scars of mammal. The level skill in the art was such that the administration of antisense oligonucleotides to nerve cells in vivo was known in the art. Example 8 provides a working example showing in vivo administration to a mammal spinal cord injury reduces GAG content. Thus, one reasonably skilled in the art could practice the invention as claimed without undue experimentation.

Claim 17 was amended to recite a method of promoting neuronal regeneration in a subject. The method includes administering an agent to a nervous system lesion to inhibit a GAG chain initiation enzyme. The agent is selected from the group consisting of antisense oligonucleotides that bind a nucleic acid sequence encoding proteoglycans, ribozymes, DNA enzymes, RNAi constructs, and small molecules. The neuronal regeneration includes neurite extension into the nervous system lesion.

Claim 17 is enabled because because one reasonably skilled in the art could make or use the invention from disclosures in the inventions coupled with information known in the art without undue experimentation.

As discussed the application provides support various agents and various methods for delivering agent to central nervous system lesions. The level skill in the art was such that the administration of antisense oligonucleotides to nerve cells in vivo was known in the art. Example 8 also provides a working example showing in vivo administration to a mammal spinal cord injury reduces promotes neuron regeneration including neurite extension in the nervous lesion. Specifically, Example 8 shows DRG cells extended processes into and around the injury cite. Moreover, the Journal of Neuroscience paper noted above indicates that administration of a DNA enzyme in accordance with Example 8 promotes axon growth in to the penumbra of the injury lesion. Thus, one reasonably skilled in the art could practice the invention as claimed without undue experimentation.

Claim 29 is enabled for a method of identifying and/or characterizing an agent capable of one or more of the following: (i) inhibiting the expression of a primary proteoglycan; (ii) inhibiting the expression and/or activity of a chain initiation enzyme; (iii) inhibiting the expression and/or activity of a chain elongation enzyme; or (iv) inhibiting the expression and/or activity of a chain sulfation enzyme. By the present amendment, Applicants have amended claim 29 to recite a method for identifying and/or characterizing an agent comprising screening a library of agents capable of one or more of the following: (i) inhibiting the expression of a primary proteoglycan; (ii) inhibiting the expression and/or activity of a chain initiation enzyme; (iii) inhibiting the expression and/or activity of a chain elongation enzyme; or (iv) inhibiting the expression and/or activity of a chain sulfation enzyme. The present application discloses numerous examples of methods for identifying and/or characterizing an

agent including, for example, cell-free assays, cell-based assays, mRNA binding assays, and *in vivo* animal models of nerve injury and nerve degeneration. Accordingly, Applicants respectively submit that amended claim 29 is enabled for a method of identifying and/or characterizing an agent comprising screening a library of agents capable of one or more of the following: (i) inhibiting the expression of a primary proteoglycan; (ii) inhibiting the expression and/or activity of a chain initiation enzyme; (iii) inhibiting the expression and/or activity of a chain elongation enzyme; or (iv) inhibiting the expression and/or activity of a chain sulfation enzyme.

Claim 31 is enabled for a method of identifying and/or characterizing an agent capable of one or more of the following: (i) reducing scar formation; (ii) promoting inter-mixing of Schwann cells and astrocytes; or (iii) promoting neurite extension. By the present amendment, Applicants have amended claim 31 to recite a method for identifying and/or characterizing an agent comprising screening a library of agents capable of one or more of the following: (i) reducing scar formation; (ii) promoting inter-mixing of Schwann cells and astrocytes; or (iii) promoting neurite extension. The present application discloses numerous examples of methods for identifying and/or characterizing an agent including, for example, cell-free assays, cell-based assays, mRNA binding assays, and *in vivo* animal models of nerve injury and nerve degeneration. Using a cell-based assay, for example, cells in culture can be contacted with one or more agents to screen for the ability of the one or more agents to promote the extension of neuronal cells in culture. Accordingly, Applicants respectively submit that claim 31 is enabled for a method for identifying and/or characterizing an agent comprising screening a library of agents capable of one or

more of the following: (i) reducing scar formation; (ii) promoting inter-mixing of Schwann cells and astrocytes; or (iii) promoting neurite extension.

Accordingly, Applicants respectively request that the 35 U.S.C. §112, first paragraph, rejection of these claims be withdrawn. Additionally, because claims 2-3, 5-6, 8-9, 12-13, 18-20, 23-28, 30, 32-34, and 36 depend either directly or indirectly from claims 1,17, 29, and 31, Applicants respectively request that the 35 U.S.C. §112, first paragraph, rejection of these claims also be withdrawn.

3. Objection to claim 1.

The Office Action objected to claim 1 because the term "GAG" is an acronym that should be clearly stated as "glycosaminoglycan (GAG)".

By the present amendment, Applicants have amended claim 1 to recite "glycosaminoglycan (GAG)". Accordingly, Applicants respectively request that the objection to claim 1 be withdrawn.

Please charge any deficiency or credit any overpayment in the fees for this matter to our Deposit Account No. 20-0090.

Respectfully submitted,

/Richard A. Sutkus/
Richard A. Sutkus
Reg. No. 43,941

TAROLLI, SUNDHEIM, COVELL,
& TUMMINO L.L.P.
1300 East Ninth Street, Suite 1700
Cleveland, Ohio 44114
Phone:(216) 621-2234
Fax: (216) 621-4072
Customer No.: 68,705

Brief Communication

A Novel DNA Enzyme Reduces Glycosaminoglycan Chains in the Glial Scar and Allows Microtransplanted Dorsal Root Ganglia Axons to Regenerate beyond Lesions in the Spinal Cord

Barbara Grimpe and Jerry Silver
Case Western Reserve University, School of Medicine, Department of Neurosciences, Cleveland, Ohio 44106

CNS lesions induce production of ECM molecules that inhibit axon regeneration. One major inhibitory family is the chondroitin sulfate proteoglycans (CSPGs). Reduction of their glycosaminoglycan (GAG) chains with chondroitinase ABC leads to increased axon regeneration that does not extend well past the lesion. Chondroitinase ABC, however, is unable to completely digest the GAG chains from the protein core, leaving an inhibitory "stub" carbohydrate behind. We used a newly designed DNA enzyme, which targets the mRNA of a critical enzyme that initiates glycosylation of the protein backbone of PGs, xylosyltransferase-1. DNA enzyme administration to TGF-β-stimulated astrocytes in culture reduced specific GAG chains. The same DNA enzyme applied to the injured spinal cord led to a strong reduction of the GAG chains in the lesion penumbra and allowed axons to regenerate around the core of the lesion. Our experiments demonstrate the critical role of PGs, and particularly those in the penumbra, in causing regeneration failure in the adult spinal cord.

Key words: proteoglycan; extracellular matrix; dorsal root ganglion; antisense; reactive astrocytes; spinal cord

Introduction

After many different types of injuries to the brain and spinal cord that open the blood–brain barrier (Fitch et al., 1999), reactive astrocytes (Menet et al., 2003) and other non-neuronal cells (Chen et al., 2002; Jones et al., 2002; Pasterkamp et al., 1999) produce various growth inhibitory molecules. Chemorepulsive keratan sulfate proteoglycans (Jones and Tuszynski, 2002) semaphorin 3A (Song et al., 1998), ephrins such as EphB2 (Bundesen et al., 2003), and slit (Brose et al., 1999) are largely confined to the lesion core. In the lesion penumbra where mesenchymal elements are lacking, various inhibitory chondroitin sulfate proteoglycans (CSPGs) are most prevalent (Snow et al., 1990; McKeon et al., 1995; Davies et al., 1999). All of these inhibitory molecules, in concert, are believed to constitute an impenetrable barrier to the passage of severed axons either through or around CNS lesions. The enzymatic digestion of just one of these components, the inhibitory glycosaminoglycan (GAG) chains of extracellular matrix PGs (McKeon et al., 1995; Bradbury et al., 2002; Pizzorusso et al., 2002; Tropea et al., 2003), is one of several key strategies that can be used to increase regeneration or sprouting of axons.

The primary enzyme that has shown efficacy in decreasing PG-mediated inhibition is bacterial chondroitinase ABC that cleaves the GAG side chains on CS-containing PGs (Bradbury et al., 2002). The use of chondroitinase ABC, however, has one major disadvantage, which is its inability to completely digest the GAG chains from the protein core. The incomplete cleavage leaves the so-called carbohydrate "stubs" behind (Caterson et al., 1985). These undigested side-chain segments, although less potently inhibitory than the complete GAG, nonetheless can reduce the capacity of axons to regenerate (Lemons et al., 2004). Therefore, an improved reagent might be one that has the ability to more completely interrupt glycosylation of the PG core protein. Targeted disruption of the enzymes that assemble the GAG chains to the protein core is one potential solution to this problem. In this paper we show that local administration of a DNA enzyme against the GAG-chain initiating enzyme, xylosyltransferase-1 (XT-1) (Goetting et al., 2000), can greatly reduce the presence of GAG chains, which normally create an inhibitory penumbra around the epicenter of spinal cord stab lesions. The reduction of fully glycosylated PGs allows for the regeneration of microtransplanted adult sensory axons around and well past the central core in our lesion model.

Materials and Methods

Preparation of primary astrocyte cultures. Astrocytes were prepared from cerebral cortices of newborn Sprague Dawley rats and cultured for 14 d in DMEM-F12 (Invitrogen, Gaithersburg, MD). The astrocytes were stimulated with TGF-β (Sigma, St. Louis, MO) at a concentration of 2 ng/μl to increase CSPG expression (Asher et al., 2000). Some cultures were also treated with 8 μM DNA enzyme or control DNA enzyme (DNA mb) for 2 d followed by fixing and immunostaining.

Immunohistochemistry: CSPG, green fluorescent protein, and GFAP. The primary astrocyte cultures were fixed, and the spinal cords were perfused with 4% paraformaldehyde (PFA). The cultures and horizontal

Received Nov. 6, 2003; revised Dec. 15, 2003; accepted Dec. 17, 2003.

This work was supported by National Institute of Neurological Disorders and Stroke Grant NS 25713, The Christopher Reeve Paralysis Foundation, The Daniel Heumann Fund, and the Brumagin Memorial Fund. We thank Albert Ries for his outstanding help in protein chemistry and photographic quantification. We also thank Prof. Paul Jones (Department of Epidemiology and Biostatistics, Case Western Reserve University) for his help in the statistical evaluation procedures.

Correspondence should be addressed to Barbara Grimpe, Case Western Reserve University, School of Medicine, Department of Neurosciences, 10900 Euclid Avenue, Cleveland, OH 44106. E-mail: bxg15@po.cwru.edu.

DOI: 10.1523/JNEUROSCI.4986-03.2004

 0270-6474/04/241393-05$15.00/0

vibratome sections through the cord (70 μm) were incubated at 37°C for 30 min followed by rinsing in PBS followed by incubation with the first antibody, the mouse monoclonal CS-56 IgM antibody (1:200; Sigma), polyclonal rabbit anti-green fluorescent protein (GFP) antibody (1:1000; Molecular Probes, Eugene, OR), or an antibody against mouse GFAP (1:500; Sigma) with 5% normal goat serum (Invitrogen) diluted in PBS and 0.1% bovine serum albumin (Sigma) overnight at 4°C on a shaker. The coverslips or cord sections were rinsed again in PBS and incubated on a shaker for 2 hr at room temperature with the second antibody, a biotin-labeled goat anti-mouse IgM (1:200; Chemicon, Temecula, CA). This was followed by rinsing the coverslips or sections in PBS and incubation for 2 hr at room temperature with Texas Red-labeled streptavidin (1:200; Molecular Probes) or an Alexa 488-labeled goat anti-rabbit or anti-mouse IgG (1:500; Molecular Probes) for the cord sections. For the primary astrocytes, Oregon Green-labeled streptavidin (1:200; Molecular Probes) was used. The tissues or cultures were then rinsed and mounted in Citifluor (Ted Pella).

To quantify the decrease in GAG staining after DNA enzyme treatment against XT-1 compared with mixed base-treated astrocyte cultures, five coverslips of each group were stained with the CS-56 antibody. The center of each coverslip was chosen grossly without first looking through the microscope objective. All fields chosen in this "blind" manner were photographed under identical conditions, and their pixel intensities were measured, averaged, and compared by Tina 2.09 (Raytest). For the statistical evaluation, the ANOVA *t* test was used.

Dot blot. Six wells of astrocytes for each group [DNA enzyme treated and control (mb) DNA enzyme treated; each 8 μM] were collected and treated in the same manner as described in Grimpe et al. (2002). Equal amounts of protein, measured by the bicinchoninic acid assay (Pierce, Rockford, IL), were diluted in Tris-buffered saline (TBS) at a concentration of 1:100, and 200 μl were loaded in the dot blot apparatus (Bio-Rad, Hercules, CA) on a nitrocellulose membrane (Bio-Rad) in a triple experiment. The membrane was incubated with the CS-56 antibody (1:500) overnight at 4°C and stained with the second antibody conjugated with horseradish peroxidase (HRP) (1:1000; Chemicon). This step was followed by an ECL reaction (Amersham Biosciences, Arlington Heights, IL). The reaction was terminated and the dot blot was developed on Hyperfilm (Amersham) after 1 min. The film was quantified by Aida v3.21 (Raytest). For further evaluation, Excel (Microsoft) was used. The dot blot was reused by incubation in stripping buffer (100 mM DTT, 2% SDS, 62.5 mM Tris-HCl, pH 6.7) at 50°C two times for 30 min, reblocked, and restained with a polyclonal rabbit anti-GFAP antibody (Accurate) in a 1:1000 dilution overnight at 4°C on a shaker. The next day the blot was rinsed three times in TBS-T (T = Tween at 0.05%) and incubated with the second HRP-conjugated antibody in a 1:1000 dilution for 2 hr at room temperature. This was followed by rinsing the dot blot three times for 30 min in TBS-T. For statistical evaluation we used the ANOVA *t* test.

Design and biotinylation of the DNA enzyme against XT-1. The DNA enzyme was designed as end-capped phosphorothioated oligodeoxyribonucleotides (ODN-PSs) with two nucleotides on each end. They were obtained from MWG Biotech. The sequence corresponded to the 3′ end of the xylosyltransferase-1 mRNA sequence (accession no. RNO295748) (Goetting et al., 2000) and included the following nucleotides: DNAXT-1as2: TGG GGG GAC TTG GGC TAG CTA CAA CGA GAC CTT G; control DNAXT-1mb2: ACG AGT CAG GAA CAT CGA TCG GGA AGT CCC ATG C. The DNA enzyme has no homology to other mammalian sequences registered in the GenBank databases of the National Institutes of Health (Altschuh et al., 1997). For the catalytic digestion of the targeted mRNA, the DNA enzyme contained a loop structure (Santoro and Joyce, 1997). The control DNA enzyme was designed not to bind to any mRNA and serves as a control for the presence of exogenous single-stranded DNA in a cell. The DNA enzyme was biotinylated at the 3′ end by MWG Biotech. Labeled DNA enzyme diffusion was evaluated in a separate group of three lesioned animals. After 7 d, spinal cord sections were stained with streptavidin-labeled Texas Red (1:200; Molecular Probes) overnight on a shaker followed by rinsing in PBS and mounting in Citifluor (Ted Pella). Evaluation of enzyme diffusion in the spinal cord tissue was measured on an Orthoplan 2 (Leitz) microscope. The same biotinylated DNA enzyme was used in our astrocyte cultures to monitor DNA enzyme uptake. The cultures were processed as described above.

Table 1. PCR conditions for XT-1, GAPDH, and cyclophilin

Name	Sequence	Length of end product	Reference
XT-1	XT1s1 5′-CTTCATCCGCCTGGGTCTTCG-3′ XT1as1 5′-GTAGTGTGTGAATTCCGCAGTGG-3′ nested XT1s2 5′-GGGCTGAGTCATCGCTACACACG-3′ nested XT1as2 5′-CGATGACATTGACAGGATCCACC-3′	316 bp	Goetting et al. (2000)
GAPDH	GAPDHs 5′-GAACATCATCCCTGCATACA-3′ GAPDHas 5′-CCAGTGAGC TTCCCGTTCA-3′	78 bp	Tajima et al. (1999)
Cyclophilin	cyclo as 5′-TGTGCCAGGGTGGTGACTT-3′ cyclo as 5′-TTTCTCTCCGTAGATGGACTT-3′	65 bp	Danielson et al. (1988)

Microtransplantation of dorsal root ganglia into the spinal cord. The adult dorsal root ganglia (DRG) were harvested from 2-month-old mice that expressed GFP under the control of the β-actin promoter (Okabe et al., 1997) using the technique described by Davies et al. (1999). Briefly, the dorsal columns of the spinal cord were exposed between the C4 and C5 vertebrae, and a small incision was made in the dura. A glass capillary with an outer diameter of ~70–90 μm was inserted 1 mm into the fasciculus gracilis and via a Picospritzer (General Valve, Fairfield, NJ); ~1×10^3 DRG in 0.5–0.9 μl of buffer was slowly injected. A dual-stab lesion was placed between the C5 and C6 vertebrae by inserting a 25 gauge needle two times into fasciculus gracilis and two times into fasciculus cuneatus ~1 mm deep. Additionally, an intrathecal catheter (PE 10; Becton Dickinson, Sparks, MD) was placed 1.9 cm into the subarachnoidal space of the spinal cord via the alanto-occipital membrane. The tubing was filled with the DNA enzyme against the XT-1 or control DNA enzyme and connected to an osmotic minipump via PE 60 tubing. The pumping rate was 0.5 μl/hr with a concentration of the DNA enzyme at 10 μg/μl over a period of 7 d. After that time the animals were killed and perfused with 4% PFA, and the spinal cords were embedded into 5% agarose/5% gelatin.

Quantification of axon regeneration: numbers of animals. In total, we used 18 DNA enzyme-treated, 6 control (mb) DNA enzyme-treated, and 12 untreated animals for our experiments. Because of variability in placement (p) of the cannula tip and successful engraftment and axonal regeneration of the DRG neurons (r), for quantification we selected only those animals in which the tubing was correctly positioned and regeneration of any axons to the vicinity of the lesion was achieved (see Fig. 2). This left a total of 6 DNA-enzyme treated (excluding 12 of 18–3p/r, -6p, -3r), 3 control (mb) DNA enzyme-treated animals (excluding 3 of 6–2p, -1r), and 6 untreated (excluding 6 of 12–6r) for our quantification.

For the quantification shown in Figure 2 and because the great number of sections exceeded our capacity for reconstructive confocal microscopy (~9 lengthy sections per animal), the number of discrete GFP+ axon fragments in each spinal cord section of all 12 experimental animals (6 DNA enzyme-treated and 6 untreated animals) was documented with the use of a Leica Orthoplan 2 microscope. An "axon fragment" was defined as any discrete piece of an axon that was stained continuously throughout the focal plane of the section. We examined an area that spanned a distance of 1 mm rostral and 2 mm caudal to the center of the lesion.

RNA isolation and PCR. Twenty-four wells, each with 100,000 stimulated astrocytes, were treated for 3 d with the DNA enzyme against XT-1 at a concentration of 8 μM. The same number of wells was used for the untreated group. Additionally, crush-lesioned spinal cords were treated for 3 d with the DNA enzyme and control (mb) DNA enzyme, and the

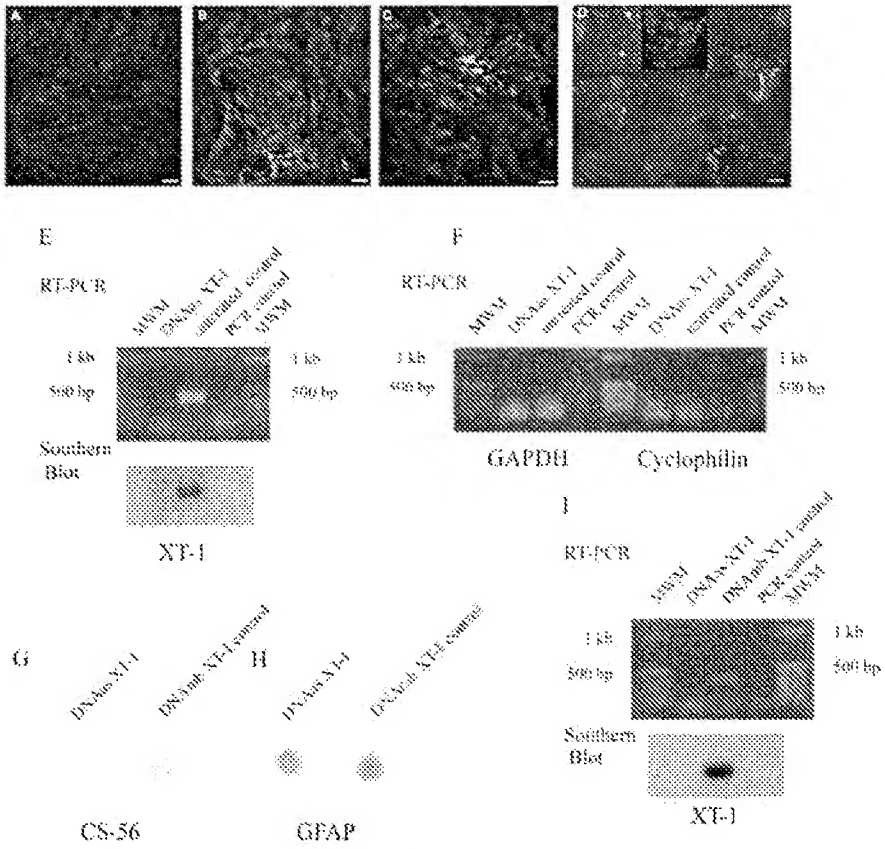

Figure 1. Confocal photomicrographs of TGF-β-stimulated primary astrocyte cultures treated with the DNA enzyme (*A*) or control DNA enzyme (*B*) or left untreated (*C*) and stained with the CS-56 antibody. Uptake of the biotin–streptavidin-labeled DNA enzyme can be seen in the astrocytes (*D*). Scale bars, 10 μm. *E*, *F*, RT-PCR–Southern blot of primary astrocyte cultures for XT-1 (*E*) and RT-PCR for GAPDH and cyclophilin (*F*) of the same mRNA. *G*, Dot blot of primary astrocyte cultures treated with the DNA enzyme or control DNA enzyme and stained with the CS-56 antibody. *H*, Restaining of the same dot blot with GFAP. *I*, RT-PCR–Southern blot for the XT-1 in a DNA enzyme- and control DNA enzyme-treated spinal cord.

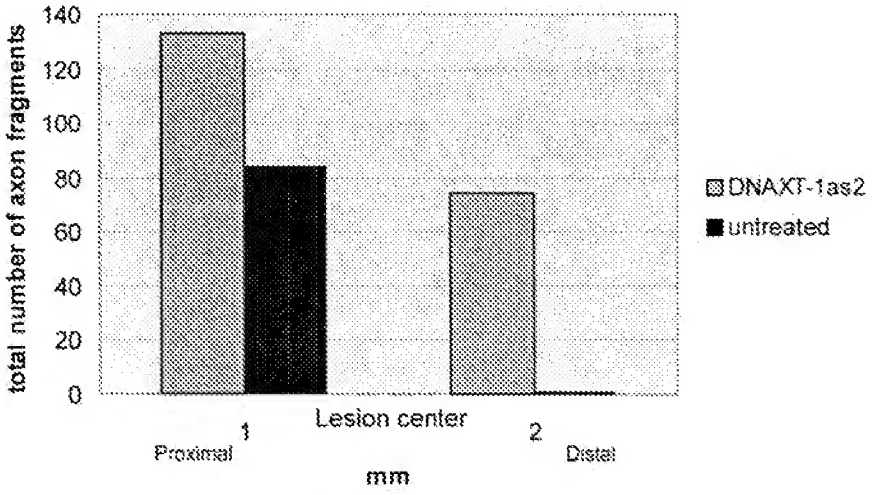

Figure 2. The histogram shows the numbers of microtransplanted DRG axon fragments proximal and distal to the lesion in DNA enzyme-treated and untreated spinal cords.

lesion site was punched out with a 3 mm diameter Uni-Punch (Premier Medical Products). The astrocytes as well as the spinal cord tissues were lysed and homogenized in Trizol (Invitrogen). Total RNA was prepared according to the supplier's protocol. Two micrograms of total astrocyte RNA and 0.6 μg of total spinal cord RNA were reverse transcribed into cDNA (Table 1) using the GenAmp RNA PCR Core Kit (PerkinElmer Life Sciences, Emeryville, CA) in accordance with the manufacturer's instructions. All RT-PCRs were analyzed on 1.0% agarose gels, stained with ethidium bromide, and photographed with a Polaroid camera (Kodak, Rochester, NY).

Southern blot analysis. The oligodeoxynucleotide XT-1 Southern blot probe (5′-CTG ACC GAT TCC AGG GCT TTC TGA TCA AGC ACC ATG TGA C-3′) (Goetting et al., 2000) was obtained from MWG Biotech. This oligodeoxynucleotide probe was digoxigenin labeled according to the manufacture's protocol (Boehringer Mannheim, Indianapolis, IN). The PCR products were electrophoretically separated on a 1.0% agarose gel. The gel was denatured for 15 min in 3 M NaCl, 0.4 M NaOH followed by a 15 min incubation in transfer solution (3 M NaCl, 8 mM NaOH) and blotted onto Hybond N+ (Amersham Biosciences) as described previously (Sambrook et al., 1989). The following day the membrane was blocked and treated according to Engler-Blum et al. (1993). As a detection reagent, CDP-Star (Boehringer Mannheim) was used. The blots were exposed to Amersham Biosciences Hyperfilm for 1–2 sec for the astrocyte preparation and 10 sec for the spinal cord preparation.

Results

To investigate the functionality of our DNA enzyme against rat XT-1 and a nonfunctional control (mb) DNA enzyme, we used TGF-β to stimulate PG upregulation in reactive astrocytes (Asher et al., 2000). We observed after staining for extracellular PGs (i.e., no Triton added) with the CS-56 antibody, which recognizes the GAG chains on CSPGs, a 2.6-fold ($p > 0.0088$; see Materials and Methods for details) decrease in staining intensity in the DNA enzyme-treated cultures versus controls (Fig. 1*A–C*). With the use of a biotin-labeled DNA enzyme, we were able to monitor enzyme uptake within the glia (Fig. 1*D*). In a nested RT-PCR experiment we show that the mRNA of XT-1 in DNA enzyme-treated astrocyte cultures is strongly reduced compared with untreated cultures (Fig. 1*E*). To confirm the specificity of our DNA enzyme, an RT-PCR of the aforementioned mRNA for glyceraldehyde-3-phosphate dehydrogenase (GAPDH) and cyclophilin was performed that showed equal amounts of the mRNAs for these "housekeeping" genes (Fig. 1*F*). A dot-blot experiment with the CS-56 antibody showed a DNA enzyme-mediated reduction in the GAG chains of PGs (Fig. 1*G*). This reduction was 1.5-fold ($p > 0.005$) compared with control DNA enzyme-treated astrocyte cultures. To document that equal amounts of total protein were loaded, the nitrocellulose membrane was stripped and restained with an anti-GFAP antibody, which resulted in comparable staining (Fig. 1*H*). The reason for the inability to see more complete reduction of the PG level in the dot-blot assay is likely attributable to the fact that the astrocytes accumulated intracellular

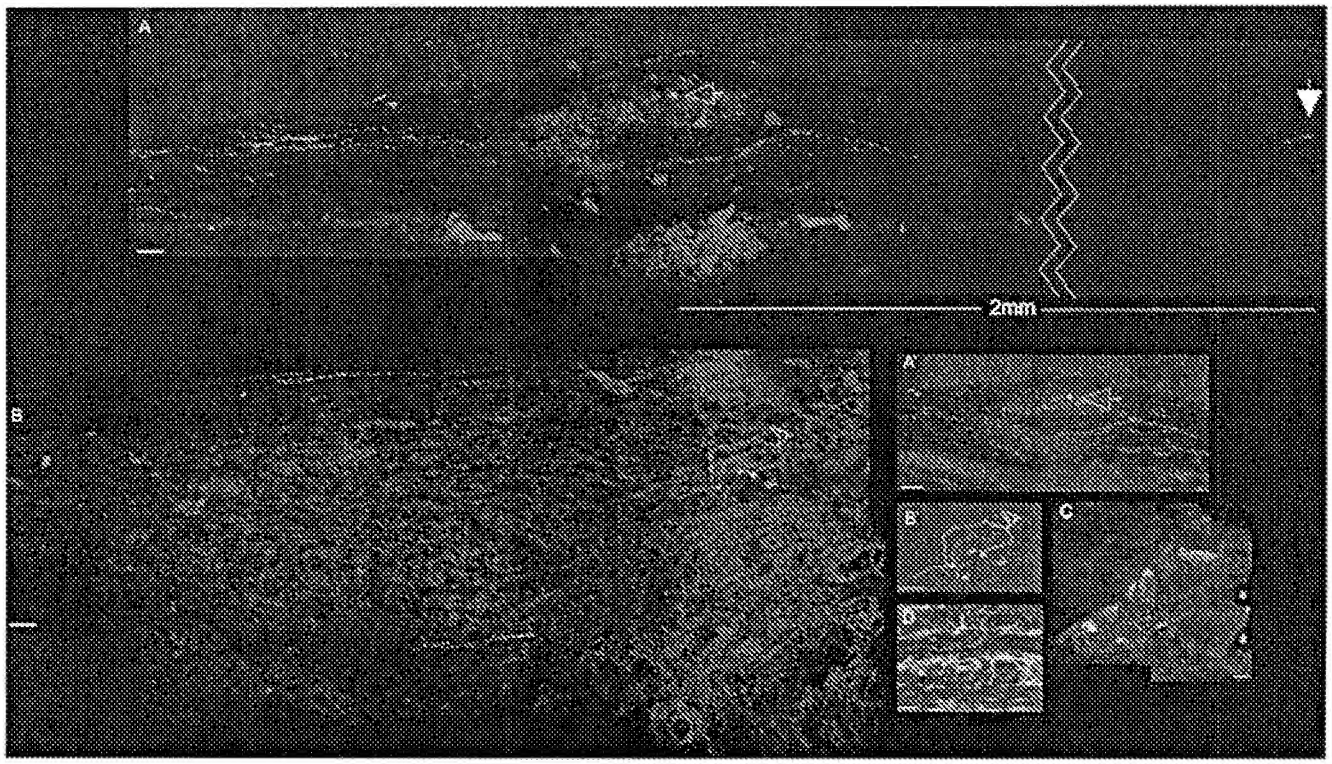

Figure 3. Confocal photomicrographs of treated and untreated spinal cords. Red/green (*A*) and green (*A'*) channels show the green DRGs and their axons passing the distinct borders of the lesion cores (red CS-56 staining) in a DNA enzyme-treated spinal cord. Axons that enter the lesion core become dystrophic (*A*, *A'*, arrows). Red/green (*B*) and green (*B'*) channels show an untreated spinal cord with the green DRG and red CS-56 staining. Note the struggling axon in the heart of the lesion. Scale bar, 50 μm. *C*, Diffusion of a labeled DNA enzyme *in vivo* 7 d after treatment. Scale bar, 100 μm. *D*, GFAP-stained section of the lesion area in a different animal. Note the disrupted astrocyte alignment in the core and borders of the lesion (L) and the aligned astrocytes (arrows) in the region where axons regenerate.

PGs before the treatment started and these were released along with extracellular PGs during the dot-blot procedure.

Microtransplantation techniques, which allow for an unambiguous identification of regenerating adult axons even within an incompletely lesioned white matter tract, have demonstrated the critical role of the lesion environment in regeneration failure (Davies et al., 1999). We repeated these experiments, and, additionally, the lesion was treated via infusion of the DNA enzyme at a concentration that was 117 times higher at the cannula tip than the concentration that was used *in vitro*. One group of control animals was treated with the control DNA enzyme and another control group was untreated. After 7 d the animals were killed, and spinal cord sections were stained for PGs with the CS-56 antibody as well as GFP to visualize the transplanted DRGs and their regenerating axons (see Fig. 3*A*,*B*). In both control groups, the rapidly regenerating axons failed to navigate beyond the confines of the lesion. Once they approached the lesion penumbra, which contains the lowest concentration of PGs (Fig. 3*B*), axons seemed trapped and were rarely able to leave this territory. Rather, just as axons behave in a PG step gradient *in vitro* (Snow and Letourneau, 1992), they preferred a path up the increasing concentration gradient of inhibitory matrix that brought them deeper into the lesion. Because the trajectory of the growth cone is documented by the shape of the axon, one gets the impression that fibers within the lesion environment have the capacity to struggle for a time, growing in contorted paths that end inevitably in the formation of dystrophic clubs (Fig. 3*B*,*B'*). In the six untreated animals, we observed 84 DRG axon fragments rostral to the lesion but just one axon fragment caudal to the lesion (Fig. 2).

In the DNA enzyme-treated spinal cords the regeneration phenotype was quite different. In six treated spinal cords, 133 axon fragments could be identified 1 mm rostral to the lesion center and 74 were found well caudal to the lesion (Fig. 2). In all of these animals the PG penumbra was variably absent. Instead, in five of these six animals a more discrete (i.e., with a sharply delineated outer edge) core of PG staining was visible very close to the original lesion site. One animal showed a complete reduction of PG staining (data not shown). In all of these animals the regenerating axons grew straight toward the lesion; however, unlike their behavior in controls, the regenerating fibers were able to maneuver very tightly around the entirety of the outside edge of the lesion core or between the paired lesions and beyond, up to distances of a maximum of 2 mm in the dorsal columns. Axons that did penetrate the lesion core formed dystrophic end balls and were unable to pass (Fig. 3*A*,*A'*). As fibers navigated around the lesion, they appeared to use regions of cord tissue in which the longitudinal geometry of the intrafascicular astroglia was relatively undisturbed (Fig. 3*D*).

A biotinylated DNA enzyme was used to assess its range of diffusion from the tip of the cannula into the cord tissue. After 7 d, labeling extended ~1 mm in all directions away from the epicenter (Fig. 3*C*). The XT-1 mRNA decrease within the lesion penumbra was also demonstrated by an RT-PCR Southern blot of treated versus control animals after 3 d (Fig. 1*I*).

Discussion

Our goal in these experiments was to test the hypothesis that the upregulation of GAG-bearing PGs after spinal cord injury plays a critical role in causing sensory axon regeneration failure. To achieve this we have used a novel DNA enzyme technology

(Grimpe et al., 2002) to disrupt a critical enzyme in the synthetic pathway of all CS-bearing PGs. Although we could demonstrate a marked reduction of CSPGs within the lesion penumbra, those CSPGs within the core of the lesion remained at much higher levels. The reasons for incomplete reduction of PG upregulation in the lesion core could be attributable to the compensatory activity of XT-2, a second enzyme that is involved with GAG-chain synthesis that may be associated with various cell types that populate the center of stab lesions (Goetting et al., 2000). Another possibility is that the stimulus for PG upregulation in the lesion core may be extremely high, thereby necessitating even greater concentrations of the DNA enzyme. It is likely that inhibitory myelin components or fibroblast-associated inhibitory molecules that are not direct targets of the DNA-enzyme may still be present in the heart of the lesion and add to its inhospitality to the regenerating fibers (Brose et al., 1999; Pasterkamp et al., 1999; Bundesen et al., 2003). The remarkable behavior, however, of the regenerating axons growing in intimate association with the perimeter of the central lesion suggests that if these molecules help to prevent regeneration in the lesion core, they must act via highly local contact-inhibitory mechanisms. Most importantly, comparison of the different behaviors of the regenerating fibers in DNA enzyme-treated versus control animals suggests that it is the geometric distribution of PG in a gradient that reaches out well beyond the center of the lesion that is especially critical in regeneration failure. Uncovering the mechanisms by which proteoglycans in the penumbra transform the growth cone into a state that appears incapable of freeing itself from the lesion environment should be a major target of future research. Finally, it is important to comment on the interesting biocatalyst activity of DNA enzymes. These new reagents, which have been used primarily in cancer and AIDS research, are relatively simple to design and have greater flexibility for selection of specific cleavage sites than ribozymes, and their synthesis is relatively inexpensive. They can provide important tools for future use in spinal cord injury research.

References

Altschuh SF, Madden TL, Schaeffer AA, Zhang J, Zhang Z, Miller W, Lipman DJ (1997) Gapped BLAST and PSI-BLAST: a new generation of protein database search programs. Nucleic Acids Res 25:3389–3402.

Asher RA, Morgenstern DA, Fidler PS, Adcock KH, Oohira A, Braistead JE, Levine JM, Margolis RU, Rogers JH, Fawcett JW (2000) Neurocan is upregulated in injured brain and in cytokine-treated astrocytes. J Neurosci 20:2427–2438.

Bradbury EJ, Moon LD, Popat RJ, King VR, Bennett GS, Patel PN, Fawcett JW, McMahon SB (2002) Chondroitinase ABC promotes functional recovery after spinal cord injury. Nature 416:636–640.

Brose K, Bland KS, Wang KH, Arnott D, Henzel W, Goodman CS, Tessier-Lavigne M, Kidd T (1999) Slit proteins bind Robo receptors and have an evolutionarily conserved role in repulsive axon guidance. Cell 96:795–806.

Bundesen LQ, Scheel TA, Bregman BS, Kromer LF (2003) Ephrin-B2 and EphB2 regulation of astrocyte-meningeal fibroblast interactions in response to spinal cord lesions in adult rats. J Neurosci 23:7789–7800.

Caterson B, Christner JE, Baker JR, Couchman JR (1985) Production and characterization directed against connective tissue proteoglycans. Fed Proc 44:386–393.

Chen ZJ, Negra M, Levine A, Ugitrin Y, Levine JM (2002) Oligodendrocyte precursor cells: reactive cells that inhibit axon growth and regeneration. J Neurocytol 31:481–495.

Danielson PE, Forss-Petter S, Brow MA, Calavetta L, Douglass J, Milner RJ, Sutcliffe JG (1988) p1B15: a cDNA clone of the rat mRNA encoding cyclophilin. DNA 7:261–267.

Davies SJ, Goucher DR, Doller C, Silver J (1999) Robust regeneration of adult sensory axons in degenerating white matter of the adult rat spinal cord. J Neurosci 19:5710–5822.

Engler-Blum G, Meier M, Frank J, Miller GA (1993) Reduction of background problems in nonradioactive Northern and Southern blot analysis enables higher sensitivity than ^{32}P-based hybridization. Anal Biochem 210:235–244.

Fitch MT, Doller C, Combs CK, Landreth GE, Silver J (1999) Cellular and molecular mechanisms of glial scarring and progressive cavitation *in vivo* and *in vitro*: analysis of inflammation-induced secondary injury after CNS trauma. J Neurosci 19:8182–8192.

Goetting C, Kuhn J, Zahn R, Brinkmann T, Kleesiek K (2000) Molecular cloning and expression of human UDP-D-xylose: proteoglycan core protein beta-D-xylosyltransferase and its first isoform XT-I. J Mol Biol 304:517–528.

Grimpe B, Dong S, Doller C, Temple K, Mafouf AT, Silver J (2002) The critical role of basement membrane-independent laminin gamma 1 chain during axon regeneration in the CNS. J Neurosci 22:3144–3160.

Jones LL, Tuszynski MH (2002) Spinal cord injury elicits expression of keratan sulfate proteoglycans by macrophages, reactive microglia, and oligodendrocyte progenitors. J Neurosci 22:4614–4624.

Lemons ML, Sandy JD, Anderson DK, Howland DR (2004) Intact aggrecan and chondroitin sulfate depleted aggrecan core glycoprotein inhibit axon growth in the adult rat spinal cord. Exp Neurol 184:981–990.

McKeon RJ, Hoke A, Silver J (1995) Injury-induced proteoglycans inhibit the potential for laminin-mediated axon growth on astrocytic scars. Exp Neurol 136:32–43.

Menet V, Prieto M, Privat A, Gimenez y Ribotta M (2003) Axonal plasticity and functional recovery after spinal cord injury in mice deficient in both glial fibrillary acidic protein and vimentin genes. Proc Natl Acad Sci USA 100:8999–9004.

Okabe M, Ikawa M, Kominami K, Nakanishi T, Nishimune Y (1997) "Green mice" as a source of ubiquitous green cells. FEBS Lett 407:313–319.

Pasterkamp RJ, Giger RJ, Ruitenberg MJ, Holtmaat AJ, De Wit J, De Winter F, Verhaagen J (1999) Expression of the gene encoding the chemorepellent semaphorin III is induced in the fibroblast component of neural scar tissue formed following injuries of adult but not neonatal CNS. Mol Cell Neurosci 13:143–166.

Pizzorusso T, Medini P, Berardi N, Chierzi S, Fawcett JW, Maffei L (2002) Reactivation of ocular dominance plasticity in the adult visual cortex. Science 298:1248–1251.

Sambrook J, Fritsch EF, Maniatis T (1989) Molecular cloning: a laboratory manual. Cold Spring Harbor, NY: Cold Spring Harbor Laboratory.

Santoro SW, Joyce GF (1997) A general purpose RNA-cleaving DNA enzyme. Proc Natl Acad Sci USA 94:4262–4266.

Snow DM, Letourneau PC (1992) Neurite outgrowth on a step gradient of chondroitin sulfate proteoglycan (CS-PG). J Neurobiol 23:322–336.

Snow DM, Lemmon V, Carrino DA, Caplan AI, Silver J (1990) Sulfated proteoglycans in astroglial barriers inhibit neurite outgrowth in vitro. Exp Neurol 109:111–130.

Song H, Ming G, He Z, Lehmann M, McKerracher L, Tessier-Lavigne M, Poo M (1998) Conversion of neuronal growth cone responses from repulsion to attraction by cyclic nucleotides. Science 281:1515–1518.

Tajima H, Tsuchiya K, Yamada M, Kondo K, Katsube N, Ishitani R (1999) Over-expression of GAPDH induces apoptosis in COS-7 cells transfected with cloned GAPDH cDNAs. NeuroReport 10:2029–2033.

Tropea D, Caleo M, Maffei L (2003) Synergistic effects of brain-derived neurotrophic factor and chondroitinase ABC on retinal fiber sprouting after denervation of the superior colliculus in adult rats. J Neurosci 23:7034–7044.

Memorandum regarding the down-regulation of GAG-chains on proteoglycans using systemic administration of the DNA enzyme to XT-1 by Barbara Grimpe

Preliminary data:

They included: intravenous administration of 2mg/kg, 6mg/kg and 10mg/kg DNA enzyme to XT-1 via the jugular vein every other day for 7 days starting immediately after moderate contusion injury. Each concentration and a control saline treated group contained 2 animals. The spinal cords were fixed and cut on a freezing microtome into 40 µm sections. The sections were systematically collected by having every 6th section in one series. One of these series was stained with the CS-56 antibody that recognizes glycosamino glycan (GAG-) chains.

After evaluation of the result by giving each section a malus (no staining) or bonus (staining) point we received data that were analyzed by Prof. Robert Duncan, a statistician, from the Department of Epidemiology and Public Health at the University of Miami and is illustrated in Table 1.

Table 1

Quantification of CS-56 immunostaining of spinal cord sections after systemic DNA enzyme to XT-1 treatment

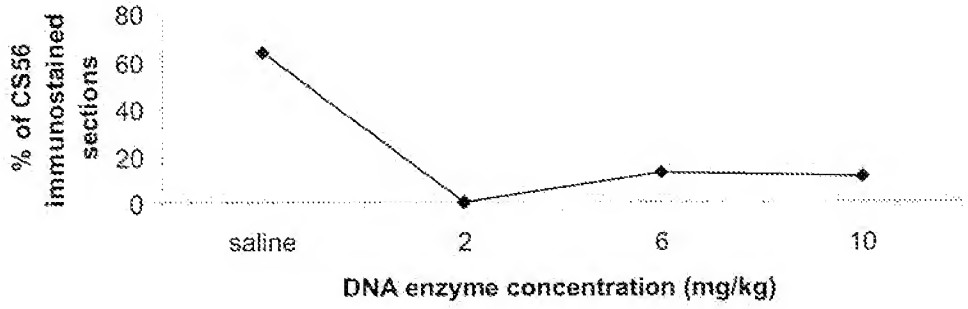

In each treatment group 2 animals were analyzed with exception of 2mg/kg DNA enzyme in which only 1 animal was survived, the other was lost based on complications generated by the contusion injury. Our data demonstrated that we have a strong reduction with the 2mg/kg concentration of our DNA enzyme because no significant difference could be observed between DNA enzyme treatment of 2mg/kg, 6mg/kg and 10mg/kg. However, there was a strong reduction in the immunostainings between saline treated animals and DNA enzyme treated animals of 2mg/kg. Therefore, two groups were generated: a) saline treated b) DNA enzyme treated group. A Chi^2-test determined a high statistical significance ($p>0.0022$) between saline treated animals (Figure A) and DNA enzyme treated animals (Figure 1B). Fisher's exact test determined also a high statistical significance between the two groups stated as $p> 0.0042$.

Confocal images were generated by starting with the saline treated animal section and adjusting all parameter. Then without changing any parameter except the depth (z-axis), images were made from a DNA enzyme to XT-1 treated animal section (Figure 1).

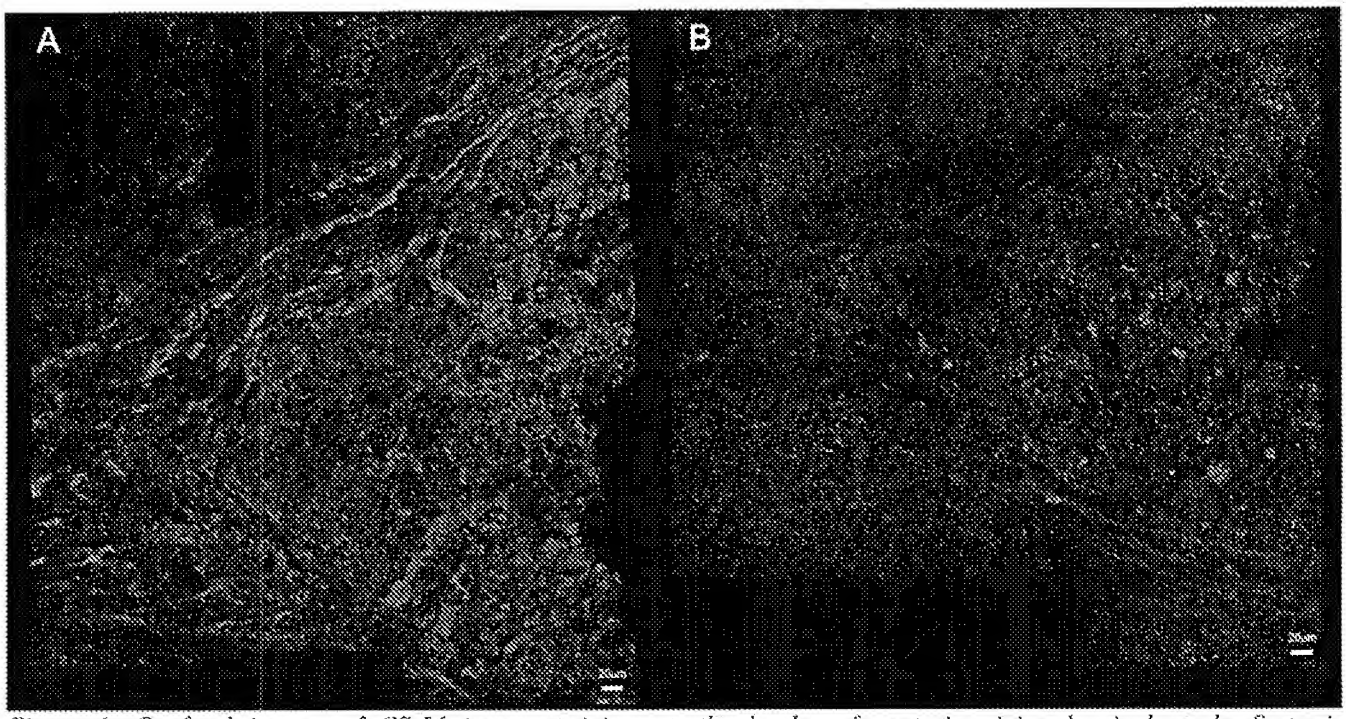

Figure 1: Confocal images of CS-56 immunostainings at the border of contusion injured spinal cords. Systemic administration of saline (A) or 10 mg/kg DNA enzyme to XT-1(B) was carried out for 7 days treated every other day.

In Figure 1 a clear difference in CS-56 immunostaining between saline (A) and DNA enzyme treated (B) animal can be observed.

In summary: Systemic administration of the DNA enzyme to XT-1 into moderate contusion injuries leads to a mark reduction in GAG-chain specific immunostainings.

PAIN

Pain 95 (2002) 143–152

www.elsevier.com/locate/pain

Inhibition of neuropathic pain by decreased expression of the tetrodotoxin-resistant sodium channel, NaV1.8

Josephine Lai[a,*], Michael S. Gold[b], Chang-Sook Kim[a], Di Bian[a,1], Michael H. Ossipov[c], John C. Hunter[c,2], Frank Porreca[a]

[a]Department of Pharmacology, University of Arizona Health Sciences Center, Tucson, AZ 85724, USA
[b]Department of OCBS, University of Maryland Dental School, Baltimore, MD 21201, USA
[c]Center for Biological Research, Roche Bioscience, Palo Alto, CA 94304, USA

Received 30 March 2001; received in revised form 10 July 2001; accepted 26 July 2001

Abstract

Neuropathic pain is a debilitating chronic syndrome that often arises from injuries to peripheral nerves. Such pain has been hypothesized to be the result of an aberrant expression and function of sodium channels at the site of injury. Here, we show that intrathecal administration of specific antisense oligodeoxynucleotides (ODN) to the peripheral tetrodotoxin (TTX)-resistant sodium channel, NaV1.8, resulted in a time-dependent uptake of the ODN by dorsal root ganglion (DRG) neurons, a selective 'knock-down' of the expression of NaV1.8, and a reduction in the slow-inactivating, TTX-resistant sodium current in the DRG cells. The ODN treatment also reversed neuropathic pain induced by spinal nerve injury, without affecting non-noxious sensation or response to acute pain. These data provide direct evidence linking NaV1.8 to neuropathic pain. As NaV1.8 expression is restricted to sensory neurons, this channel offers a highly specific and effective molecular target for the treatment of neuropathic pain. © 2002 International Association for the Study of Pain. Published by Elsevier Science B.V. All rights reserved.

Keywords: Tetrodotoxin-resistant sodium current; Neuropathic pain; Antisense; Dorsal root ganglia; Sensory neurons; Peripheral neuron type 3 sodium channel (PN3); Sensory neuron-specific sodium channel (SNS); Voltage sensing sodium channel type 1.8 (NaV1.8)

1. Introduction

Chronic pain is a major symptom of peripheral neuropathies whether induced by AIDS, cancer chemotherapy, diabetes, or by direct physical trauma to the peripheral nerves (Bennett, 1994; Scadding, 1994; Portenoy, 1996). Such neuropathic pain is often highly debilitating and resistant to therapeutic intervention. Animal models of neuropathic pain have suggested that a prominent feature in the maintenance of the neuropathic state is an abnormal, persistent hyperexcitability of the sensory afferent neurons within the peripheral nerve following injury (Wall and Gutnick, 1974; Devor, 1994; Matzner and Devor, 1994). A common clinical finding is that broad-spectrum sodium channel blockers, represented by local anesthetics such as lidocaine (Tanelian and Brose, 1991; Backonja, 1994; Hunter and Loughhead, 1999) can acutely suppress neuropathic pain. The relative contribution of individual sodium channel subtypes in neuropathic pain remains unclear. However, the biophysical properties of a tetrodotoxin (TTX)-resistant sodium channel, NaV1.8 (Goldin et al., 2000), formerly PN3/SNS (Akopian et al., 1996; Sangameswaran et al., 1996), make this channel a likely candidate for maintaining the sustained, repetitive firing of the peripheral neuron following injury (Elliott and Elliott, 1993; Rush et al., 1998). Importantly, the expression of NaV1.8 is restricted to the periphery in sensory neurons of the dorsal root ganglia (DRG) (Akopian et al., 1996; Sangameswaran et al., 1996), suggesting that a blockade of this channel might allow relief from neuropathic pain with minimal side effects. However, this possibility cannot be tested pharmacologically because currently available sodium channel blockers do not distinguish between sodium channel subtypes. In an earlier study, we have employed the strategy of antisense oligodeoxynucleotide (ODN) targeting of NaV1.8 expression in an animal model of neuropathic pain to test this hypothesis (Porreca et al., 1999). The data indicated that a selective 'knock-down' of NaV1.8 protein in the DRG neurons by specific antisense

* Corresponding author. Tel.: +1-520-626-2147; fax: +1-520-626-4182.
E-mail address: lai@u.arizona.edu (J. Lai).
[1] Present address: Department of Neurobiology, Amgen Inc., Thousand Oaks, CA 91360, USA.
[2] Present address: CNS and CV Research, Schering-Plough Research Institute, Kenilworth, NJ 07033, USA.

PII: S0304-3959(01)00391-8

ODN to NaV1.8 prevented the hyperalgesia and allodynia caused by spinal nerve ligation (SNL) injury (Kim and Chung, 1992). The data implicate a pathophysiological role of NaV1.8 in peripheral neuropathy.

Here, we present new evidence that validate the specific functional disruption of NaV1.8 in sensory neurons by the antisense ODN treatment in vivo. This study demonstrates that ODN accumulates in DRG cells upon intrathecal (i.th.) administration in a time-dependent manner, resulting in a 'knock-down' of the NaV1.8 protein by the antisense ODN to NaV1.8, but not by the mismatch ODN or by saline. This 'knock-down' of the NaV1.8 protein in the DRG cells correlates with both a reduction in the TTX-resistant sodium conductance in the DRG cells as well as a reversal of neuropathic pain in SNL rats. These data suggest that a blockade of NaV1.8-mediated sodium currents may underlie the anti-allodynic and anti-hyperalgesic effects of the antisense ODN to NaV1.8 in SNL rats, and provide further evidence that NaV1.8 is likely to be an effective target for the treatment of neuropathic pain.

2. Materials and methods

2.1. Animals

Adult male Sprague–Dawley rats (150–300 g) were used for the experiments. All surgical procedures employed in this study were reviewed and approved by the University of Arizona Institutional Care and Use Committee. Animal care and handling were in accordance with the Guide for the Care and Use of Laboratory Animals as adopted and promulgated by the National Institutes of Health.

2.2. ODNs that target NaV1.8

An antisense sequence ('antisense I': 5′-TCCTCT-GTGCTTGGTTCTGGCCT-3′) complementary to nucleotides 107–129 of the coding region of the rat NaV1.8) and a corresponding mismatch sequence ('mismatch I': 5′-TC-CTTCGTGCTGTGTTCGTGCCT-3′) were synthesized as phosphodiester ODNs using standard *O*-cyanoethylphosphoramidite chemistry (Midland Certified Reagent Co., Midland, TX, USA). A second antisense sequence to NaV1.8 ('antisense II': 5′-CCACGGACGCAAAGGGGA-GCT-3′), and its corresponding mismatch sequence ('mismatch II': 5′-CCAGCGACGACAAGGGAGGCT-3′), were also synthesized. The mismatch sequences were derived from the respective antisense sequences by scrambling six bases, giving rise to a 25% mismatch with the target sequences. This level of mismatch was sufficient to abolish the selectivity of the ODN for the target sequence (Wahlestedt, 1994). These sequences were screened against the Genbank Database using the BLAST (basic local alignment search tool) algorithm with an expectation value set at 1000 for short sequence search (the search excluded STS (sequence tagged site) and EST (expressed sequence tag). Search result indicated that there was no significant complementarity (equal or greater than 70% as defined by the mismatch control) with known sequences for other ion channels. The fluorescence labeling of antisense I and mismatch I was carried out by conjugation of the fluorophor carboxytetra-methyl-rhodamine, *N*-hydroxysuccinamide ester to the 5′ end of the ODN, and the fluorescence-labeled ODNs were purified by reverse phase high-performance liquid chromatography (HPLC) (Midland Certified Reagent Co., Midland, TX, USA). All ODNs were reconstituted in nuclease-free ultrapure water to a final concentration of 9 μg/μl.

2.3. Administration of ODNs

Chronically indwelling i.th. catheters were implanted into rats according to the method described by Yaksh and Rudy (1976) for ODN administration. The animals were allowed to recover from the implantation surgery for 3–5 days prior to any experimentation, and monitored daily after surgery for signs of motor deficiency. Intrathecal injections of ODNs or saline were made in a volume of 5 μl followed by a 9 μl saline flush.

2.4. Evaluation of the uptake of ODN by DRG cells

The fluorescence-labeled ODN was injected i.th. as a single bolus injection of 45 μg. At 2, 4, 8, or 12 h after ODN administration, rats were deeply anesthetized with ketamine and perfused transcardially with 200 ml of phosphate buffered saline (PBS, pH 7.4) containing heparin (1500 IU/l), followed by 500 ml of cold 4% paraformaldehyde. The L4 and L5 lumbar DRGs were dissected and cryoprotected with 30% sucrose in nuclease-free PBS overnight at 4°C. Frozen sections (20–40 μm) were thaw-mounted onto glass slides and coverslipped with Vectorshield (Vector, Burlingame, CA, USA). Fluorescence images were acquired using a Hamamatsu C5810 color charged couple device (CCD) camera attached to a Nikon E800 microscope. Standard optics for rhodamine (TRITC) included a 25-nm band pass excitation filter centered at 540 nm and a 60-nm band pass emission filter centered at 630 nm. The digitized output of the camera was acquired with Metamorph image analysis software (Universal Imaging Corporation, West Chester, PA, USA) on a Pentium microcomputer.

2.5. Western transblot analysis

Crude membranes were prepared from DRGs by homogenization in ice-cold 10 mM PBS/100 μM phenylmethylsulfonylfluoride/50 μg/ml bacitracin/30 μM bestatin/10 μM captopril, and were solubilized with ice-cold 10 mM PBS, pH 7.4, containing 2% Triton X-100, 4% sodium dodecyl sulphate (SDS), and protease inhibitor cocktail as above. Proteins were separated by SDS-polyacrylamide gel electrophoresis (SDS-PAGE) and transblotted onto nitrocellulose

membranes (BioRad, Hercules, CA, USA). For the immunostaining of NaV1.8, we used a monoclonal antibody for rat NaV1.8 (9D11C8, 1:50) (Okuse et al., 1997), an horseradish peroxidase (HRP)-conjugated anti-mouse IgG sheep antiserum as secondary antibody (1:1000, Amersham, Piscataway, NJ, USA) and processed for chemiluminescence detection (ECL, Amersham, Piscataway, NJ, USA). After each immunodetection, the transblots were stripped by incubating 2 × 10 min in 100 mM 2-mercaptoethanol/2% SDS/62.5 mM Tris HCl, pH 6.7, at 50°C, and were then stored at 4°C in wet-sealed bags or processed for the immunostaining of vanilloid receptor-1 (VR1) or nerve growth factor receptor (trkA). For the immunostaining of VR1, we used a rabbit antiserum for rat VR1 (1:1000). This antiserum was raised against the carboxyl terminus of VR1 as described previously (Tominaga et al., 1998). The blots were washed and incubated with a HRP conjugated anti-rabbit IgG goat antiserum (80 ng/ml, Jackson Immunoresearch, West Grove, PA, USA) and processed for chemiluminescence detection. The antiserum labels a single band at 93 kDa in DRG extracts. For the immunostaining of trkA, a rabbit antiserum for rat trkA (1:1000; Chemicon, Temecula, CA, USA) was used. The antiserum labels two major bands, one at 110 kDa and one at 140 kDa. The 110 kDa band, which is the more prominent of the two, is used for densitometry.

A direct comparison between DRG extracts from saline, mismatch I, or antisense I treated rats were carried out by processing these samples in parallel under identical conditions. Chemiluminescent labeling of transblots was detected by optimal exposure to Hyperfilm (Amersham, Piscataway, NJ, USA). The films were scanned at 600 dpi. Scanned images were analyzed by Metamorph image analysis software (Universal Imaging Corporation, West Chester, PA, USA) on a Pentium microcomputer. For densitometric analysis of each image, a fixed size rectangular box was placed on each labeled band and the integrated optical density (IOD) was determined for each band (expressed in arbitrary units). The IOD of NaV1.8 from the mismatch or antisense treated samples was expressed as a percent of the IOD of NaV1.8 from the saline control and corrected by the loading factor derived from VR1 ($[IOD]_{saline}/[IOD]_{sample}$) or similarly from trkA. Each DRG extract was prepared from eight lumbar DRGs from two rats. Two extracts were prepared for each of the treatments and analyzed independently.

2.6. Electrophysiological analysis

Surgical procedures and dissociation protocol were similar to that described previously (Gold et al., 1996a) except for two differences. First, ganglia were incubated in culture medium containing collagenase at 37°C and bubbled with carbogen, shortening the enzyme treatment time by 50% (i.e. to 45 min). Second, 1 h after plating, neurons were transferred from a humidified incubator at 37°C and 3% CO_2, to HEPES buffered L-15 media and stored at room temperature. Neurons were studied between 2 and 7 h after removal from the animal. Voltage-clamp recordings were performed using an HEKA EPC9 (HEKA Electonik., Lambrecht/Pfaz Germany). Data were low-pass filtered at 5–10 kHz with a 4-pole Bessel filter and digitally sampled at 25–100 kHz. Capacity transients were cancelled and series resistance was compensated (>80%); a P/4 protocol was used for leak subtraction. Electrodes (0.7–3 MΩ) were filled with (in mM): 100 CsCl, 40 tetraethylammonium-Cl, 5 NaCl, 1 $CaCl_2$, 2 $MgCl_2$, 11 EGTA, 10 HEPES, 2 Mg–ATP, 1 Li–GTP; pH was adjusted to 7.2 with TRIS-base, osmolarity was adjusted to 310 mOsm. Bath solution used to record whole cell Na^+ currents in isolation contained (in mM): 35 NaCl, 30 tetraethylammonium-Cl, 65 choline-Cl, 0.1 $CaCl_2$, 5 $MgCl_2$, 10 HEPES, 10 glucose, pH adjusted to 7.4, osmolarity adjusted to 325 mOsm. Voltage-gated Ca^{2+} currents were recorded by adding 2.5 mM Ca^{2+} to this solution. TTX-resistant I_{Na} was isolated from TTX-sensitive Na^+ currents with a 500 ms pre-pulse to −50 mV. This voltage-step is also a potential at which the persistent TTX-resistant currents are inactivated (Cummins et al., 1999), such that the TTX-resistant I_{Na} reflects the activation of NaV1.8.

After formation of a tight seal (>5 GΩ) and compensation of pipette capacitance with amplifier circuitry, whole cell access was established. Five hyperpolarizing pulses (10 ms, 20 mV from −60 mV) were recorded for use in the determination of the cell capacitance. Whole cell capacitance and series resistance was compensated with the amplifier circuitry. High-threshold voltage-gated Ca^{2+} currents were evoked from a holding potential of −60 mV. The holding potential was then changed to −80 mV. Voltage-gated Na^+ currents were evoked following a 500 ms voltage-step to either −120 or −50 mV. Current evoked from −50 mV was considered to be TTX-resistant current (Gold et al., 1996b), while the difference between the current evoked from −120 and −50 mV was considered to be TTX-sensitive current. Application of TTX (250 nM) to five cells confirmed that these voltage-clamp protocols were sufficient to isolate the two currents. Current density was determined by dividing the peak current evoked at 0 mV by the cell capacitance. Three groups of rats were studied: antisense I treated, mismatch I treated, and saline-treated. Three rats were studied in each group and 12–20 neurons were studied from each rat. To accommodate for animal variability, parameters obtained for each neuron were pooled to generate a mean parameter for each animal. Statistical analyses were performed on the mean of the means (i.e. $n = 3$ for each group).

2.7. Animal model of neuropathic pain

The surgical procedure for L5/L6 SNL was carried out according to that described by Kim and Chung (1992). Sham-operated control rats were prepared in an identical fashion except that the L5/L6 nerve roots were not ligated. The behavior of the rats was monitored carefully for any visual indication of motor disorders, change in weight, or

general health. ODNs were administered to the rats from day 5 to 10 post-surgery.

2.8. Evaluation of tactile allodynia and thermal hyperalgesia

Mechanical allodynia was determined by measuring the paw withdrawal threshold to probing with a series of calibrated (0.4–15 g) von Frey filaments (Chaplan et al., 1994). Thermal hyperalgesia was determined by measuring paw withdrawal latencies to a radiant heat source applied to the plantar surface of the affected paw of nerve-injured or sham-operated rats (Hargreaves et al., 1988). Statistical analysis of the data involved analysis of variance (ANOVA) followed by Fisher's Least Significant Difference test. The baseline latency to paw withdrawal in response to von Frey probing or thermal stimulus was determined for each animal prior to surgery and thereafter monitored once daily.

2.9. Evaluation of acute nociception

Acute, high threshold thermal nociception was elicited by dipping the distal half of the tail into a water bath maintained at 52°C and recording the latency to a rapid tail-flick, or by exposure of the paw to a radiant heat source applied through a glass floor maintained at 30°C as described above. The maximum time allowed was 10 s for the tail-flick response and 40 s for the paw-flick response in order to prevent tissue damage. For high-threshold mechanical stimulation, the dorsum of the hindpaw was exposed to increasing pressure applied by a blunt probe (Randall–Sellito test, Ugo-Basile) and the response threshold recorded in arbitrary units.

2.10. Immunohistochemistry

At the appropriate time, the animals were deeply anesthetized with 10% chloral hydrate (300 mg/kg) and perfused intracardially with 500 ml of 0.1 M PBS followed by 500 ml of a solution of 10% formalin in 0.1 M PBS. The L4, L5, and L6 DRG were removed and processed for paraffin embedding. Paraffin embedded DRG sections were cut at 4 μm, deparaffinized, and rehydrated in xylene followed by immersion in ethanol gradient. Tissue sections were incubated with a rabbit anti-NaV1.8 antiserum (1:600)(Novakovic et al., 1998), followed by a biotinylated donkey anti-rabbit secondary antibody (1:500, Jackson Immunoresearch, West Grove, PA, USA) and a strepavidin-Cy3 solution (1:4000, Jackson Immunoresearch, West Grove, PA, USA). The specificity of the primary antibody was determined by pre-absorption with the corresponding synthetic peptide or omission of primary antibody. Because staining intensity might vary between experiments, sections from normal non-operated animals were used as standards and included in each run of staining. Statistical analysis was performed using a two-sample *t*-test comparing the SNL + NaV1.8 antisense ODN group to saline controls and when comparing the SNL + saline or SNL + NaV1.8 mismatch ODN to the normal, non-operated group.

3. Results

In order to ascertain the delivery of the ODNs into the DRG cells, antisense I was covalently labeled with carboxytetramethylrhodamine and delivered as a single bolus i.th. injection (45 μg) to the lumbar region of the spinal cord where the DRG lie intradurally, continuous with the cerebrospinal fluid. The time course of the uptake of the labeled ODN by the lumbar DRGs was then monitored by fluorescence microscopy. Fig. 1A depicts a representative cross-section of a DRG in which cells are visualized by Nissl stain. Neuronal cell bodies are distinguished by their round cell shape. DRG from saline injected control rats exhibited low level of autofluorescence seen as punctate, endosomal staining in neuronal cell bodies (Fig. 1B). Few neuronal cell bodies exhibited fluorescence level that was significantly above that seen in saline injected control at 2 h after ODN injection (data not shown). However, by 4–8 h after ODN injection, many cell bodies were highly fluorescent (Fig. 1C), and this fluorescence labeling was maintained in neuronal cells 12 h after the bolus injection (Fig. 1D). The fluorescence intensity appeared to be variable among the cell bodies irrespective of cell size, suggesting that not all the cells took up ODN with equal efficiency, and that the labeling was not due to some non-specific diffusion or optical artifact. The progressive increase in the fluorescence associated with the DRG cells indicates that the uptake of the ODN occurred in a time-dependent manner and was detectable within 4–8 h. The fluorescence was

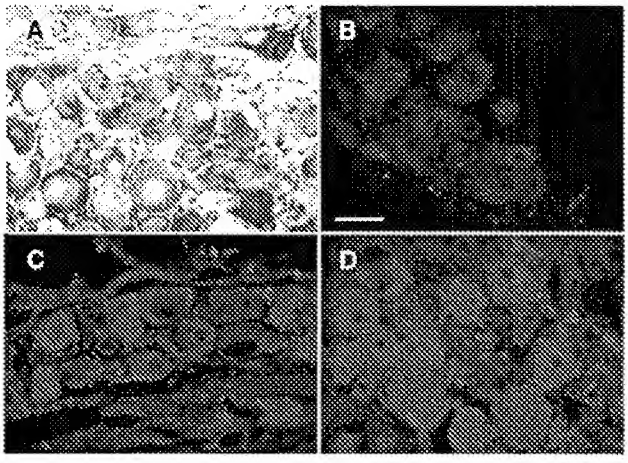

Fig. 1. The distribution of fluorescence-tagged NaV1.8 antisense I in the lumbar DRGs after a single i.th. injection of 45 μg of the tagged ODN. (A) Transmitted light micrograph of a representative cross-section of a DRG. The cells are visualized with Nissl staining. (B–D) Fluorescence micrographs of DRG from saline control (B), or taken 8 h (C), and 12 h (D) after the tagged ODN injection. The fluorescence images of the DRG sections were collected using a 40 × objective lens and a standardized exposure time of 3 s. Images are representative of lumbar DRGs from two rats for each time point. Scale bar denotes 50 μm.

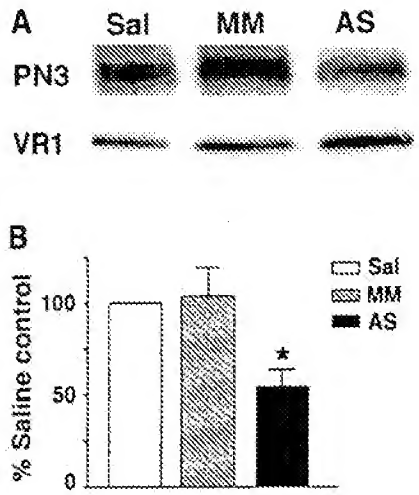

Fig. 2. Western analysis of NaV1.8 and VR1 in DRG extracts after saline, mismatch I (MM), or antisense I (AS) treatment. (A) The monoclonal antibody for NaV1.8 labels predominantly a high molecular weight protein of >200 kDa; the antiserum for VR1 labels a single band of 93 kDa. The transblot is representative of four independent analyses. (B) Relative intensities of NaV1.8 immunolabeling in the samples using that in the saline control as 100%, and corrected for loading by the relative intensities of VR1 immunolabeling in the samples ($N = 4$). The relative intensity of NaV1.8 from AS-treated DRG is significantly different (*) from that in MM-treated DRG ($P < 0.05$; unpaired t-test).

observed primarily in the cytoplasm of these cell bodies and was distributed throughout the cytoplasm. This intracellular distribution of the antisense ODN is amenable to its mode of action, which presumably may be through a selective hybridization to the messenger RNA that encodes NaV1.8, located in the cytoplasm. This selective hybridization may disrupt the translation of the target transcripts by the antisense ODN, resulting in a reduction, or 'knock-down', of the expression of the NaV1.8 protein.

A 'knock-down' of NaV1.8 by antisense I was determined by Western immunoblotting analysis of DRG from saline, antisense I, or mismatch I treated rats (Fig. 2). The densitometric analysis of the NaV1.8 immunoreactivity was standardized against that of two unrelated proteins that are expressed in DRG cells: the capsaicin receptor VR1 and the nerve growth factor receptor trkA. It was found that repeated i.th. injection (45 μg per injection, twice daily for 3 days) of antisense I, but not mismatch I, significantly reduced the NaV1.8 immunoreactivity in DRG extracts when compared with that of saline control rats using VR1 as internal loading standard (Fig. 2A). Densitometric analysis showed that the level of NaV1.8 immunoreactivity in antisense I treated DRGs was 55 ± 8% when compared with saline control, and was significantly different from that in the mismatch I treated DRGs (Fig. 2B). Densitometric analysis using trkA as internal loading standard yielded a similar reduction in the level of NaV1.8 immunoreactivity (NaV1.8 labeling was 60% that of saline control), further substantiating the antisense-I mediated 'knock-down' of the NaV1.8 protein. Thus antisense I selectively and significantly reduced NaV1.8 expression in the DRG after 3 days of repeated i.th. administration.

The consequence of this 'knock-down' of NaV1.8 on its function was determined by measuring the current density of I_{Na} in acutely dissociated DRG cells from saline, antisense I, or mismatch I treated rats. For these experiments, rats were treated with saline, antisense I, or mismatch I as for Western analysis, with the exception that the last two ODN injections for either antisense I or mismatch I consisted of the same ODN sequence that had been covalently labeled with carboxytetramethylrhodamine. Under epifluorescence illumination, a sub-population of neurons exhibited a relatively high level of cytoplasmic fluorescence indicative of ODN uptake. These neurons were studied electrophysiologically. For the saline-treated animals, a randomly chosen population of sensory neurons with

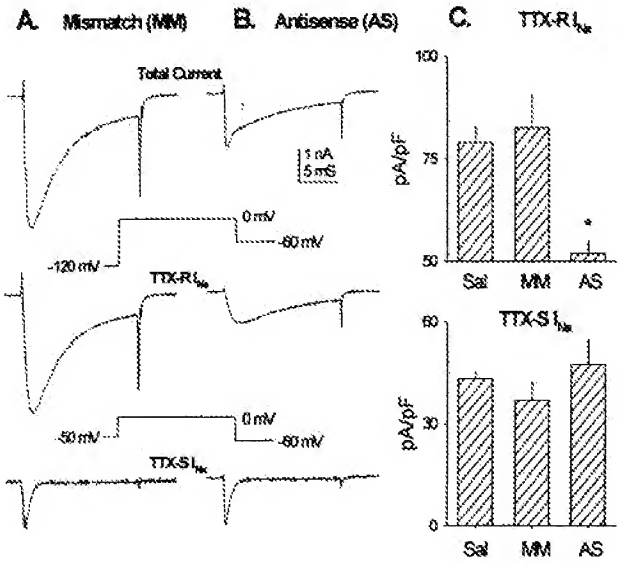

Fig. 3. NaV1.8 antisense ODN selectively reduces TTX-resistant Na^+ current. (A) Voltage-gated sodium currents recorded from a DRG neuron from a mismatch I (MM) treated rat. Top panel: voltage-gated Na^+ current evoked following a 500 ms pre-pulse to −120 mV. The voltage-clamp protocol used to evoke the currents is shown beneath the current traces. Middle panel: TTX-resistant Na^+ current was isolated by changing the pre-pulse amplitude to −50 mV. To ensure that the pre-pulse protocol was sufficient to isolate TTX-sensitive from TTX-resistant Na^+ current, a group of neurons was studied utilizing both the pre-pulse protocol and 250 nM TTX to isolate the Na^+ currents. Currents isolated with these two methods were identical (data not shown). The −50 mV pre-pulse step is a potential at which the persistent TTX-resistant currents are inactivated, such that the remaining TTX-resistant Na^+ current reflects the activation of $Na_V1.8$. Bottom panel: TTX-sensitive Na^+ current was isolated as the difference between the current evoked from −120 mV and the current evoked from −50 mV. (B) Voltage-gated Na^+ currents recorded in a DRG neuron from an antisense I (AS) treated rat. Current traces in the top, middle, and bottom panels were obtained as described in (A). (C) The density of TTX-R I_{Na} (top panel) was significantly reduced in neurons from AS-treated rats compared to neurons from MM or saline-treated rats ($P = 0.01$, one-way ANOVA with Tukey post hoc). There was no difference between groups with respect to the density of TTX-sensitive Na^+ currents (bottom panel). Values are mean ± SEM of the mean values determined for each rat; $N = 3$ for each group.

small cell-body diameters was studied. Importantly, administration of antisense I selectively and significantly attenuated TTX-resistant voltage-gated Na^+ currents (Fig. 3). TTX-resistant current density (pA/pF) in the antisense I treated group was 35% less than that observed in the mismatch I, or saline-treated groups. The difference between the antisense I treated group and the other two groups was due to a change in TTX-resistant current rather than cell-body capacitance because there was no significant difference in mean cell-body capacitance between groups (30.4 ± 0.77, 32.7 ± 1.71, and 29.9 ± 0.68 pF for saline, mismatch I, and antisense I groups, respectively).

The TTX-resistant current remaining in the DRG cells after antisense I treatment has the same biophysical properties as the TTX-resistant current in cells from saline or mismatch I treated rats. In this regard, there was no difference between groups in the threshold for current activation (i.e. between −35 and −30 mV), the voltage of peak inward current (0 mV), or the rate of inactivation at peak inward current (5.8 ± 2.1, 6.2 ± 2.6, and 5.7 ± 1.8 ms for saline, mismatch ODN, and antisense I treated neurons, respectively). There was a small but significant difference in the voltage-dependence of activation between antisense I treated and mismatch I treated rats with respect to the voltage of half maximal activation (−8.9 ± 2.4 and −6.7 ± 3.0 mV, for mismatch I and antisense I treated rats, respectively). However, there was no difference between antisense I and saline-treated rats (−8.7 ± 2.3 mV, $P > 0.05$, one-way ANOVA). Furthermore, there was no difference between groups with respect to the slope factor, describing the change in conductance for e-fold change in voltage (5.4 ± 0.6, 5.1 ± 0.6, and 5.2 ± 0.7 mV, for saline, mismatch I, and antisense I treated neurons, respectively; $P > 0.05$, one-way ANOVA). Hence, antisense I treatment had no effect on the biophysical properties of the TTX-resistant I_{Na} remaining in the DRG neurons. As additional controls for the specificity of antisense treatment, we assessed the influence of antisense administration on voltage-gated Ca^{2+} currents and TTX-sensitive voltage-gated Na^+ currents. Antisense I treatment had no significant effect on either high threshold voltage-gated Ca^{2+} currents (112.6 ± 48.7, 93.7 ± 51.9, and 93.3 ± 47.6 pA/pF for saline, mismatch ODN, and antisense ODN treated rats, respectively) or the TTX-sensitive voltage-gated Na^+ currents (Fig. 3) when compared to either saline or mismatch I treated groups ($P > 0.05$, one-way ANOVA).

The functional consequences of 'knock-down' of NaV1.8 protein by antisense I was also evaluated by determination of the response thresholds to nociceptive stimuli. At no time during treatment with either antisense or mismatch ODN (non-labeled or fluorescence-labeled) were any overt behavioral, particularly in the central nervous system (CNS), side effects observed; animals gained weight, behaved normally, and displayed no motor deficiencies as evaluated visually and on a rotarod. The absence of any abnormal behavioral characteristics during ODN treatment shows that the dosage of the ODN used and the various sequences employed in this study did not precipitate any non-specific, sequence-independent, ODN-mediated signs of behavioral toxicity. An absence of NaV1.8 immunoreactivity in the CNS and cardiac tissue obviates any physiological consequence of a functional 'knock-down' of NaV1.8 in these organ systems. Neither antisense I nor mismatch I altered the response of non-operated or sham-operated rats to acute nociceptive mechanical or thermal stimuli in the paw pressure (Randall–Sellito), tail-flick (hot-water), or paw-flick (radiant heat) tests (Fig. 4A,B). Additionally, neither antisense nor mismatch ODN to NaV1.8 had any effect on non-noxious threshold responses in sham-operated or saline-treated rats.

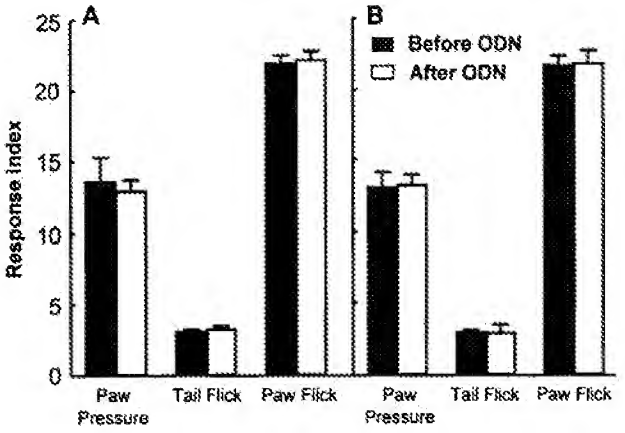

Fig. 4. Neither antisense I (A) nor mismatch I (B) ODN produced changes in response thresholds to acute nociception induced by pressure or thermal stimuli. Rats received twice daily injections (45 μg, i.th.) of either mismatch I or antisense I for 2 days and again on the morning of day 3. On the afternoon of day 3, the rats were tested for nociceptive responses to blunt force applied to the dorsum of the paw (Randall–Selito test), the 52°C hot water tail-flick test, and to radiant heat applied to the plantar surface of the paw (Hargreaves test). Response index indicates the latency (s) for the tail-flick and paw-flick tests and arbitrary response units derived from the Randall–Sellito apparatus used. The responses the rats exhibited after ODN injections were not significantly different ($P > 0.05$) than those obtained from the same animals prior to the injection of the ODNs ($N = 6$ per group).

The possibility that NaV1.8 'knock-down' may influence neuropathic pain states was assessed using the SNL injury model. SNL, but not sham-surgery, produced a state of tactile allodynia and thermal hyperalgesia within 3 days of surgery consistent with that previously described (Chaplan et al., 1997; Wegert et al., 1997; Nichols et al., 1995). Treatment with mismatch I had no significant effect on the level of tactile allodynia observed in the SNL rats; paw withdrawal thresholds on the side ipsilateral to the injury remained in the allodynic range throughout the course of the study (Fig. 5A). In contrast, administration of antisense I caused a significant elevation in paw withdrawal thresholds on the side ipsilateral to the nerve ligation by the end of the second day of treatment. Paw withdrawal thresholds of antisense I treated SNL rats did not differ significantly from saline, mismatch I, or antisense I treated sham-operated rats, but were significantly higher than the thresholds seen in

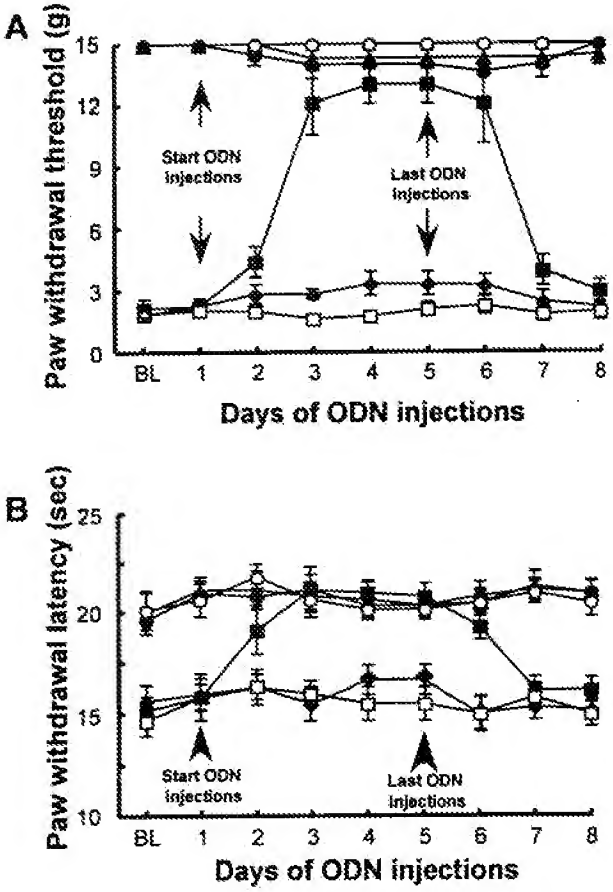

Fig. 5. Antisense, but not mismatch, ODN to NaV1.8, administered by twice daily i.th. injections (45 μg) to rats with a SNL injury (tight ligation of L5 and L6 spinal nerves distal to the DRG) reversed established tactile allodynia (A) and thermal hyperalgesia (B). Saline, antisense I, or mismatch I were given for 5 days to sham-operated or nerve-injured rats. The administration began 5 days after sham or nerve ligation surgery. Only the NaV1.8 antisense significantly reversed the developed tactile allodynia (A), measured by paw withdrawal threshold to probing with von Frey filaments, or thermal hyperalgesia (B), measured by decreased paw withdrawal latency to a noxious radiant heat stimulus directed to the plantar surface of the hindpaw. Both tactile allodynia and thermal hyperalgesia were reversed by approximately 48 h after the antisense ODN administration. The hyperesthesia returned on the second day after the last NaV1.8 antisense ODN injection. $N = 6$ rats per group. Sham-operated, saline (open circles); SNL, saline (open squares); sham-operated, antisense ODN (closed circles); SNL, antisense ODN (closed squares); sham-operated, mismatch ODN (closed triangles); SNL, mismatch ODN (closed diamonds); BL, baseline.

mismatch I treated SNL rats. Elevated paw withdrawal thresholds were observed while the antisense I treatment was maintained, i.e. for 4 days, indicating a reversal of established tactile allodynia (Fig. 5A). A similar profile was observed with respect to reversal of thermal hyperalgesia (Fig. 5B). Pre-antisense I treatment levels of tactile allodynia (Fig. 5A) and thermal hyperalgesia (Fig. 5B) were re-established by the end of the second day after the cessation of ODN treatment, demonstrating that the effect of antisense I was reversible. A second antisense ODN sequence, antisense II, and its corresponding control, mismatch II, were also investigated in the SNL injury model. This additional NaV1.8 antisense, but not mismatch, ODN, produced a reversal of established tactile allodynia and thermal hyperalgesia in a manner similar to that observed with antisense I (data not shown). Again, the effects of antisense II were completely reversible.

The distribution of NaV1.8-immunoreactivity (NaV1.8-IR) in the L4, L5, and L6 DRGs in normal and nerve-injured rats and the effect of NaV1.8 mismatch and antisense ODN treatment on the expression of the NaV1.8 protein in these DRGs was assessed using immunohistochemistry in conjunction with confocal microscopy. In normal non-operated rats, NaV1.8-IR protein was observed predominantly in the small diameter neurons of the L4 DRG (83.2% of all small diameter cells <700 μm^2, 17.2% of all medium to large diameter cells >700 μm^2, $n = 3$,) as previously described (Novakovic et al., 1998), and a similar percentage of small and large neurons were labeled in the L5 and L6 DRG (Figs. 6 and 7). Following SNL, the relative propor-

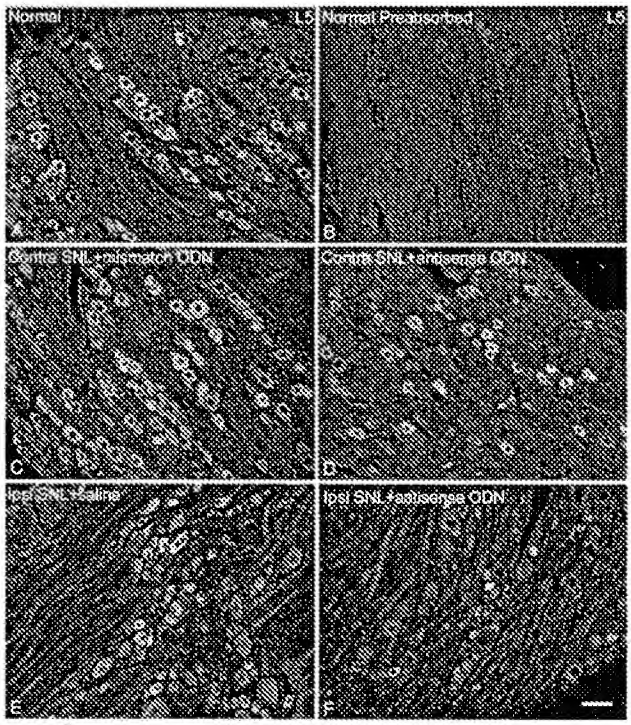

Fig. 6. Confocal photomicrographs of NaV1.8-immunoreactivity (NaV1.8-IR) in L5 DRG neurons from normal (A, B) and SNL animals (C–F). In the normal, non-operated animal NaV1.8-IR was expressed by the majority of small diameter neurons and a minority of large diameter neurons (A). NaV1.8-IR was abolished when an excess of the NaV1.8 peptide antigen was included in the immunoreaction (B). In SNL animals that received mismatch I, DRG contralateral to the SNL showed a comparable number of NaV1.8-IR neurons (C) as that in normal animals (A), whereas SNL animals that received antisense I showed a significant reduction of NaV1.8-IR in both small and large DRG neurons in the contralateral DRG (D). In the ipsilateral DRG from SNL animals, there was a reduction in the number of small but not large DRG neurons that expressed NaV1.8-IR (E). In SNL animals that received antisense I, there was a significant reduction in the number of both small and large neurons expressing NaV1.8-IR (F). Scale bar, 50 μm.

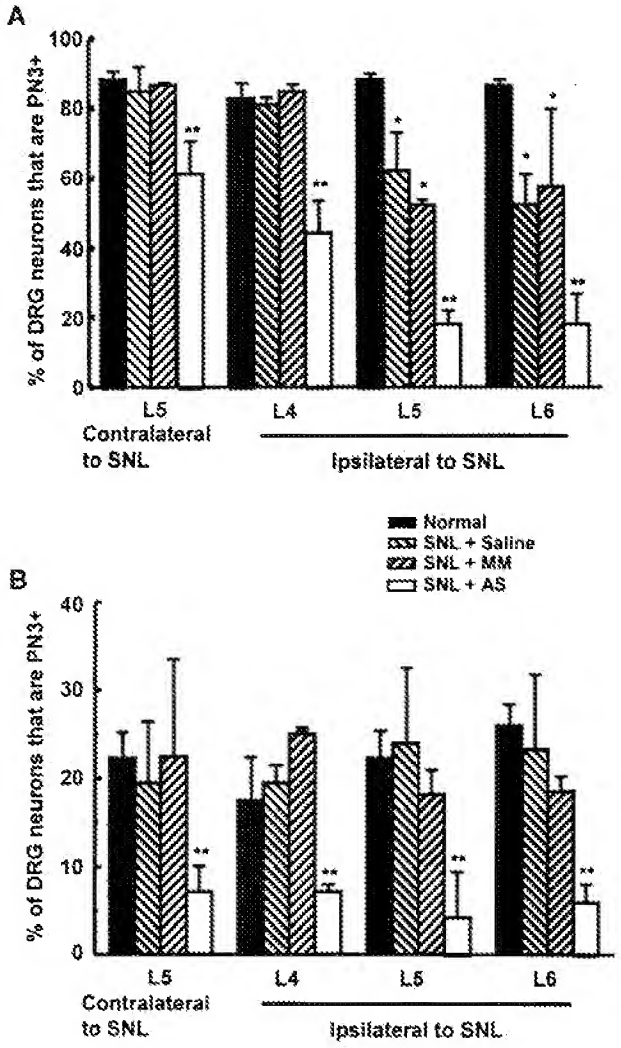

Fig. 7. Quantification of NaV1.8-immunoreactivity (NaV1.8-IR) in the L4, L5, and L6 DRGs of normal, non-operated animals and animals undergoing SNL. In the L4, L5, and L6 DRGs obtained from normal, non-operated animals, approximately 80% of the small (A) and 20% of the large (B) DRG neurons expressed NaV1.8-IR. SNL followed by i.th. infusion of saline resulted in a reduction in the number of small diameter neurons that expressed NaV1.8-IR in the L5 or L6 DRGs but not the L4 DRG (A) and no change in the number of large diameter neurons expressing NaV1.8-IR in the L4, L5, or L6 DRG (B). In animals that received SNL followed by infusion of mismatch I, the number of neurons in the L4, L5, and L6 DRG that expressed NaV1.8-IR was not significantly different from animals that received SNL followed by infusion of saline. In contrast, SNL followed by infusion of antisense I resulted in a significant reduction in the number of small (A) and large (B) DRG neurons that expressed NaV1.8-IR as compared to normal animals or animals that received SNL followed by infusion of saline or mismatch ODN.

tion of neurons showing NaV1.8-IR was significantly altered and the change was dependent upon the level of the DRG (Figs. 6 and 7). While the number of small neurons that expressed NaV1.8-IR in the L5 and L6 DRG decreased to 63 and 53%, respectively, following SNL, the percentage of neurons expressing NaV1.8 protein was not significantly changed in either small diameter neurons in L4 DRGs or large diameter neurons in L4/5/6 DRGs (Fig. 7). In SNL animals, after 48 h of i.th. injections of saline or NaV1.8 mismatch ODN, there was no significant change in the percentage of small diameter neurons or large diameter neurons as compared to SNL followed by saline injection (Figs. 6 and 7). In contrast, in animals which received SNL followed by NaV1.8 antisense ODN injection, there was a significant 'knock-down' of NaV1.8 protein in L4/5/6 DRGs when evaluated at either the ipsilateral (relative to the SNL injury) or contralateral sides (Figs. 6 and 7). Thus, in DRGs from SNL rats treated with NaV1.8 antisense ODN, the percentage of small diameter neurons expressing NaV1.8 at DRG levels L4/5/6 was 44, 18, and19%, respectively, and the percentage of large diameter neurons expressing the NaV1.8-IR at DRG levels L4/5/6 was 7, 4, and 5%, respectively (Fig 7). These data substantiate the conclusion that the anti-allodynic and anti-hyperalgesic effect of NaV1.8 antisense ODN was due to a selective 'knock-down' of NaV1.8.

4. Discussion

In the present study, we have demonstrated that i.th. administration of ODNs provides an effective mode of delivery of these molecules to the DRG neurons in vivo. Repeat i.th. injection of an antisense ODN designed to target transcripts for the TTX-resistant sodium channel subtype, NaV1.8, results in a significant reduction of the NaV1.8 protein as well as the density of TTX-resistant sodium current in the DRG, while the mismatch control has no effect. This reduction in the TTX-resistant sodium current after antisense ODN treatment is based on comparing currents with similar properties from each treatment group. These currents closely resemble those described by Rush et al. (1998) as TTX-R1 and by Vogel and coworkers (Scholz et al., 1998) as the slow TTX-R current, and are distinct from the persistent currents described by Cummins et al. (1999), the fast TTX-R currents described by Vogel and coworkers (Scholz et al., 1998), or the TTX-R2, TTX-R3, or TTX-R4 described by Rush et al. (1998). Furthermore, this reduction in the TTX-resistant sodium current after antisense ODN treatment correlates with an uptake of the tagged ODN by the DRG cells, and is dependent on the sequence-specificity of the antisense ODN because a similar uptake of the tagged mismatch ODN by DRG neurons has no effect on the TTX-resistant sodium current in these cells. The specificity of the antisense ODN for NaV1.8 is further substantiated by the finding that this ODN has no effect on the density of voltage-sensitive calcium current, or the TTX-sensitive sodium current in the same cells. In addition, previous data from our laboratories have shown that treatment with this antisense ODN for NaV1.8 does not alter the expression of other sodium channel subtypes, including PN1 and PN4 (Porreca et al., 1999).

When this antisense ODN is given to rats which have been subjected to L5/L6 SNL injury, the animals exhibit a reversal

of behavioral signs of neuropathic pain; subsequent immunohistochemical analysis of the DRG from these animals confirmed a 'knock-down' of the NaV1.8 immunoreactivity in the lumbar DRG. That the anti-allodynic and anti-hyperalgesic effect of the antisense ODN treatment is due to a specific 'knock-down' of NaV1.8 is validated by several control experiments. First, treatment with a mismatch ODN sequence has no effect on the allodynia and hyperalgesia in SNL rats; correspondingly, there is no reduction in the immunoreactivity of NaV1.8 in the lumbar DRG from these mismatch ODN treated rats. Second, the behavioral effect of the antisense ODN treatment is time related and reversible, i.e. the neuropathic pain states return upon the cessation of the antisense ODN treatment in the SNL rats. The time course for the onset and reversibility of the antisense ODN effect is consistent with the reported 26 h half-life for the rate of sodium channel turnover and biosynthesis (Waechter et al., 1983). Third, a second antisense ODN to NaV1.8 also produces similar anti-allodynic and anti-hyperalgesic effects in SNL rats, and such effects are also reversible. Collectively, the data from the protein, biophysical and behavioral analyses provide strong evidence that i.th. antisense ODN to NaV1.8 consistently and specifically elicits a reduction of NaV1.8 protein expression in the DRG. Such reduction results in a decrease in the slow TTX-R current in the DRG, and reverses the behavioral manifestation of nerve injury induced pain, suggesting that there is a direct link between NaV1.8 channel activity and neuropathic pain states after peripheral nerve injury.

An important aspect of the antisense ODN effect in vivo is that thresholds to non-noxious tactile and noxious thermal stimuli in the nerve-injured animals are reversed to, but not above, the control (i.e. mismatch ODN or sham-surgery) range. Moreover, no changes are observed in response to probing with non-noxious, or noxious stimuli in sham-operated rats that are treated with the antisense ODN. This suggests that a 'knock-down' of NaV1.8 protein expression does not alter normal non-noxious or noxious sensory thresholds, thus NaV1.8 channel activity appears to contribute little to normal sensory thresholds. The negligible effect of the antisense ODN to NaV1.8 on normal noxious sensory thresholds is in general agreement with the moderate changes in response to noxious stimuli observed in NaV1.8 'knock-out' mice (Akopian et al., 1999). These mutant mice exhibit a small increase in latency to certain nociceptive tests including tail pressure and warm water tail-flick tests, but no change in response to the hot plate test when compared with the wild type mice. The mutant mice also show similar threshold to non-noxious stimuli as the wild type mice. Thus, although the 'knock-out' mice have a complete deletion of NaV1.8 compared with a partial depletion of the channel protein after antisense ODN treatment, the overall effect of NaV1.8 deletion on normal sensory thresholds is still small. Further, because NaV1.8 'knock-out' mice exhibit a compensatory up-regulation of the TTX-sensitive sodium channel, PN1, in the C-fibers, this could also account for the observed changes in nociceptive latency in these mutant mice. Such compensatory changes do not appear to occur following antisense ODN administration (Porreca et al., 1999; Khasar et al., 1998).

A similar experimental approach found that i.th. NaV1.8 antisense ODN also reduced the hyperalgesia and allodynia that are associated with tonic inflammation induced by complete Freud's adjuvant (Porreca et al., 1999), and the hyperalgesia induced by prostaglandin E2 (Khasar et al., 1998), but had no effect on the hyperalgesia and allodynia associated with the acute inflammation induced by 2% carrageenan (measured 3 h after carrageenan injection) (Porreca et al., 1999). Tonic inflammatory hyperalgesia is associated with an enhanced activity of NaV1.8 (England et al., 1996; Gold et al., 1996b; Cardenas et al., 1997) and may correspond to an increase in NaV1.8 transcript (Tanaka et al., 1998). Thus, a 'knock-down' of NaV1.8 protein by antisense ODN treatment to normalize the up-regulation of NaV1.8 function may explain the anti-hyperalgesic effect of NaV1.8 antisense ODN treatment. L5/L6 SNL injury, on the other hand, is associated with a moderate reduction in the number of small diameter cell bodies that express NaV1.8 in the injured L5 (Figs. 6 and 7). This observation is consistent with previous findings in the lumbar DRGs after chronic constriction injury of the sciatic nerve (Novakovic et al., 1998). A reduction of NaV1.8 transcript in the injured L5 and L6 DRGs was also apparent after SNL (Okuse et al., 1997). Therefore, in these peripheral neuropathy models, the contribution of the NaV1.8 channel activity to the maintenance of neuropathic pain does not appear to be directly related to an enhanced synthesis of NaV1.8 in the injured nerve. Instead, NaV1.8 activity is likely to be up-regulated through other post-translational regulatory mechanisms such as the distribution of the channel proteins (Novakovic et al., 1998) or protein phosphorylation (England et al., 1996). In addition, recent evidence suggests that aberrant activity in uninjured nerves may contribute to neuropathic pain (Li et al., 2000). In this regard, the normal expression of NaV1.8 in either small or large cells in the adjacent uninjured L4 nerve fibers (Fig. 7) could contribute to such abnormal input. As NaV1.8 antisense treatment reduces the expression of NaV1.8 in both injured and uninjured nerve fibers, these findings suggest that a continual expression of NaV1.8 channel activity in injured and/or adjacent uninjured nerve fibers is necessary for the maintenance of neuropathic pain.

In summary, we have demonstrated that 'knock-down' of NaV1.8 protein elicits an anti-allodynic and anti-hyperalgesic effect as well as a decrease in TTX-R current. This effect of NaV1.8 antisense ODN is time- and dose-dependent, sequence-specific, reversible and well-defined because it does not precipitate behavioral toxicity, and is without effect on normal non-noxious or noxious sensory functions. Together these data suggest that a selective inhibitor of NaV1.8 expression or function may offer pain relief in neuropathy. Critically, given the restricted expression of NaV1.8 to sensory neurons the effect of inhibition of